UNIVERSIDADE FEDERAL DO RIO GRANDE DO SUL
INSTITUTO DE CIÊNCIAS BÁSICAS DA SAÚDE
PROGRAMA DE PÓS-GRADUAÇÃO EM NEUROCIÊNCIAS

Daniel Prato Schmidt

DESCRIÇÃO MORFOMÉTRICA DO NERVO MASSETÉRICO EM CADÁVERES HUMANOS E A SUA RELAÇÃO ANATÔMICA COM A ARTÉRIA MASSETÉRICA

Porto Alegre

2019

CIP - Catalogação na Publicação

Schmidt, Daniel Prato
Descrição Morfométrica do Nervo Massetérico em Cadáveres Humanos e sua Relação Anatômica com a Artéria Massetérica / Daniel Prato Schmidt. -- 2019.
88 f.
Orientadora: Taís Malysz.

Coorientador: Taís.

Dissertação (Mestrado) -- Universidade Federal do Rio Grande do Sul, Instituto de Ciências Básicas da Saúde, Programa de Pós-Graduação em Neurociências, Porto Alegre, BR-RS, 2019.

1. Nervo massetérico. 2. Fibra nervosa. 3. Anatomia. 4. Histologia. 5. Morfometria. I. Malysz, Taís, orient. II. , Taís, coorient. III. Título.

Elaborada pelo Sistema de Geração Automática de Ficha Catalográfica da UFRGS com os dados fornecidos pelo(a) autor(a).

Daniel Prato Schmidt

DESCRIÇÃO MORFOMÉTRICA DO NERVO MASSETÉRICO EM CADÁVERES HUMANOS E A SUA RELAÇÃO ANATÔMICA COM A ARTÉRIA MASSETÉRICA

Dissertação submetida ao Programa de Pós-Graduação em Neurociências da Universidade Federal do Rio Grande do Sul como requisito parcial para a obtenção do título de Mestre.

Orientadora: Profª Drª Taís Malysz

Porto Alegre

2019

Dedico este trabalho à

Universidade Federal de Santa Maria (UFSM)

"A forma é a imagem plástica da função"

(Ângelo Ruffini, 1925)

AGRADECIMENTOS

A minha família, em especial aos meus pais Elizabeth e Sérgio pela sólida formação dada até minha juventude que me proporcionou a continuidade nos estudos até a chegada a este mestrado, e aos meus irmãos Adriana e André, pelo apoio, incentivo e compreensão constantes na busca dos meus objetivos. A todos vocês meus eternos agradecimentos!

Em especial a minha amada Universidade Federal de Santa Maria (UFSM) pelo apoio dado à minha qualificação profissional.

A minha querida orientadora Taís, por toda sua dedicação, compreensão, amizade, pela confiança em mim depositada, pelos conselhos, questionamentos e discussões que ajudaram na realização deste trabalho.

Aos Técnicos em Anatomia e Necropsia da Universidade Federal do Rio Grande do Sul Douglas e Leonardo pela disponibilidade em ajudar e atender minhas solicitações. Em especial ao Biólogo Antônio pelo total interesse em auxiliar nos trabalhos desenvolvidos no departamento.

Aos Técnicos em Laboratório Maikel e Chris pela ajuda no processamento das amostras do estudo. Em especial a Técnica Silvia por ser sempre um exemplo para mim de profissional ética, competente e responsável.

Aos colegas do Departamento de Morfologia da Universidade Federal de Santa Maria, em especial ao Ruben, amigo e colega de trabalho de longa data, por assumir minhas atribuições durante o período do mestrado.

A Professora Denise, coordenadora do PPGNeurociências, por abrir as portas do programa para mim e orientar nos caminhos a serem seguidos sempre com muita sabedoria e atenção.

A Sra. Andréa e aos demais integrantes da secretaria de pós-graduação, pelas inúmeras ajudas solicitadas por mim neste período, e que foram sempre eficazmente atendidas.

Aos membros da banca, pela leitura e exame da presente dissertação.

Agradeço, enfim, a Universidade Federal do Rio Grande do Sul pela oportunidade.

Sumário

LISTA DE ABREVIATURAS

SNP - Sistema nervoso periférico

SNC - Sistema nervoso central

NM - Nervo massetérico

AM - Artéria massetérica

g-ratio - Grau de mielinização

AST - Área de secção transversal

I - Nervo olfatório

II - Nervo óptico

III - Nervo oculomotor

IV - Nervo troclear

V - Nervo trigêmeo

VI - Nervo abducente

VII - Nervo facial

VIII - Nervo vestibulococlear

IX - Nervo glossofaríngeo

X - Nervo vago

XI - Nervo espinal acessório

XII - Nervo hipoglosso

V_1 - Ramo oftálmico do nervo trigêmeo

V_2 - Ramo maxilar do nervo trigêmeo

V_3 - Ramo mandibular do nervo trigêmeo

AMI - Artéria maxilar interna

Manuscrito 1

MN - Masseteric nerve

MA - Masseteric artery

CSA - Cross-sectional area

SMAS - Superficial muscular aponeurotic system

V_3 - Mandibular branch of trigeminal nerve

IMA - Internal maxillary artery

MbMA - Masseteric branch of maxillary artery

Manuscrito 2

MN - Masseteric nerve

g-ratio - Degree of myelination

SMAS - Superficial muscular aponeurotic system

NGF - Nerve growth factor

ROI - Region of interest

LISTA DE TABELAS

Manuscrito 1

Manuscrito 2

LISTA DE FIGURAS

Manuscrito 1

Manuscrito 2

RESUMO

Introdução: O nervo massetérico (NM) tem sido utilizado em anastomoses massetérico-faciais na correção da paralisia facial, tanto de origem central, quanto periférica por ser uma técnica cirúrgica que apresenta baixa morbidade. Entretanto, esta prática ainda é pouco difundida pelo fato dos cirurgiões terem dificuldade em acessar e localizar o nervo. **Objetivos**: Descrever morfometricamente o nervo massetérico em cadáveres humanos e a sua relação anatômica com a artéria massetérica (AM). **Material e métodos**: Foram dissecadas 24 hemifaces de 12 cadáveres formolizados (6 homens e 6 mulheres), do acervo do Laboratório de Anatomia Humana da Universidade Federal do Rio Grande do Sul (UFRGS), Brasil. O NM e a AM foram identificados em cada hemiface, na sua posição ao cruzar a incisura mandibular, e a localização anatômica dessas estruturas foram descritas através da distância horizontal e vertical a pontos anatômicos superficiais de referência (trago e arco zigomático, respectivamente) e através da mensuração da profundidade em relação ao arco zigomático, através de um paquímetro digital Vonder® 150 mm. Um fragmento do nervo (3 mm), ou do ramo principal no caso de haver ramos secundários, foi retirado, fixado em solução de glutaraldeído 2,5% e submetido ao protocolo padrão de inclusão em resina acrílica. Cortes semifinos transversais (900nm) foram obtidos através do ultramicrótomo e corados em azul de toluidina 1%. Um corte de cada nervo foi selecionado, a imagem capturada e analisada através do software Zeiss ZenBlue 2.3. Os dados morfométricos microscópicos coletados foram: área de seção transversal (AST), diâmetro total e número de fascículos do nervo, número total de fibras mielinizadas, área média das fibras mielinizadas e dos axônios, diâmetro médio das fibras mielinizadas e dos axônios, espessura de bainha de mielina e grau de mielinização (g-ratio). Além disso, test t de Student foi utilizado para comparar as variáveis entre homens e mulheres e entre os lados direito e esquerdo das faces ($p<0,05$). Os resultados foram expressos em média±desvio-padrão. **Resultados**: O NM cruzou a incisura mandibular, anteriormente e superiormente à AM através de 1 (79,1%), 2 (12,5%) ou 3 (8,3%) ramos para suprir a porção profunda do músculo masseter. A distância média do NM ao trago foi de 33,24±3,1 mm e a partir do arco zigomático foi de 8,34±2,1 mm. As hemifaces direitas apresentaram maior distância do NM (34,5±2,1 mm *vs*. 31,9±2,8 mm; $p<0,05$) e da AM (32,29±2,51 mm *vs*. 29,86±2,62 mm; $p<0,05$) em relação ao trago.O NM esteve posicionado cerca de 2,17±1,24 mm anterior e 1,78±1,79 mm superior à AM. A distância horizontal entre o NM e a AM foi menor em homens (1,53±0,74 mm *vs*. 2,81±1,33 mm, $p<0,05$). A profundidade média do NM em relação ao arco zigomático foi 11,32±2,1 mm, sendo que esta foi maior em cadáveres homens (12,43±2,21 mm *vs.* 10,22±1,26 mm; $p<0,05$). O NM foi identificado como monofascicular com 1683±315 fibras nervosas mielínicas, a AST média foi 0,30±0,1 mm² e o diâmetro médio do nervo foi 0,76±0,18 mm. A área média de fibras e de axônios foi de 51,85±30,58 μm² e 12,98±11,48 μm², respectivamente. O diâmetro médio das fibrase o axonal foram de 7,65±2,74 μm e 3,7±1,7 μm, respectivamente. A média da espessura da bainha de

mielina foi de 1,98±0,82 µm e a média do g-ratio foi de 0,48±0,11. O NM apresentou 12,5% de pequenas, 9,33% de médias e 78,17% de grandes fibras mielinizadas. O MN apresentou 21,08% de fibras com diâmetro menor que 5 µm, 77,05% de fibras com diâmetro entre 5-12 µm e 1,9% de fibras com diâmetro maior que 12 µm. As hemifaces direitas apresentaram menores valores ($p<0,05$) que as esquerdas para área axonal (11,10±8,58 µm *vs*. 15,08±13,75 µm), diâmetro axonal (3,46±1,48 µm *vs*. 3,96±1,88 µm) e g-ratio (0,45±0,10 *vs*. 0,51±0,11). A espessura de bainha de mielina foi maior no lado direito (2,09±0,84 µm *vs*. 1,85±0,77 µm, $p<0,05$). Os resultados mostraram valores semelhantes na comparação entre os lados para área e diâmetro de fibras nervosas ($p>0,05$). **Conclusões**: Os dados obtidos neste estudo contribuem para a identificação de uma região de localização do nervo massetérico para acesso cirúrgico e fornecem dados morfométricos microscópicos para nortear procedimentos de anastomose massetérico-facial em correções cirúrgicas de paralisias da musculatura da mímica facial.

Palavras-chave: Nervo massetérico; artéria massetérica; morfometria macroscópica; morfometria microscópica.

ABSTRACT

Introduction: The masseteric nerve (MN) has been used in masseteric-facial anastomoses in the correction of facial paralysis, both of central and peripheral origin because it is a surgical technique that presents low morbidity. However, this practice is still less widespread because surgeons have difficulty accessing and locating the nerve. **Objectives**: The objectives of this study are to describe morphometrically the masseteric nerve in human cadavers and its anatomical relationship with the masseteric artery (MA).**Material and methods**: Twenty-four hemifaces of 12 formolized cadavers (6 men and 6 women) from the Human Anatomy Laboratory of the Universidade Federal do Rio Grande do Sul (UFRGS), Brazil, were dissected. The MN and MA were identified in each hemiface, in their position crossing the mandibular notch, and the anatomical location of these structures were described through the horizontal and vertical distance to superficial reference anatomical points (tragus and zygomatic arch, respectively) and the depth measurement in relation to the zygomatic arch, through a Vonder® 150 mm digital caliper. A fragment of the nerve (3 mm), or the main branch in the case of secondary branches, was removed, fixed in 2.5% glutaraldehyde solution and submitted to the standard inclusion protocol in acrylic resin. Cross sections (900 nm) were obtained through the ultramicrotome and stained in 1% toluidine blue. A slice of each nerve was selected, the image captured and analyzed using Zeiss ZenBlue software 2.3edition. The microscopic morphometric data collected were: cross section area (CSA), total diameter and number of nerve fascicles, total number of myelinated fibers, mean area of myelinated fibers and axons, mean diameter of myelinated fibers and axons, myelin sheath thickness and degree of myelination (g-ratio). In addition, Student's t test was used to compare the variables between men and women and between the right and left sides of the faces ($p<0.05$). Results were expressed as mean±standard deviation. **Results**: The MN crossed the mandibular notch, anteriorly and superiorly to MA, through 1 (79.1%), 2 (12.5%) or 3 (8.3%) branches to supply the deep portion of the masseter muscle. The mean distance from MN to the tragus was 33.24±3.1 mm and from the zygomatic arch was 8.34±2.1 mm. The right hemifaces presented a greater distance from the MN (34.5±2.1 mm *vs*. 31.9±2.8 mm, $p<0.05$) and MA (32.29±2.51 mm *vs*. 29.86±2.62 mm, $p<0.05$) in relation to the tragus. The MN was positioned about 2.17±1.24 mm anterior and 1.78±1.79 mm superior than the MA. The horizontal distance between MN and MA was lower in men (1.53±0.74 mm *vs*. 2.81±1.33 mm, $p<0.05$). The mean depth of the MN in relation to the zygomatic arch was 11.32±2.1 mm, which was higher in male cadavers (12.43±2.21 mm *vs*. 10.22±1.26 mm, $p<0.05$). The MN was identified as monofascicular with 1683±315 myelinated nerve fibers, the mean CSA was 0.30±0.1 mm² and the mean nerve diameter was 0.76±0.18 mm. The mean fiber area was 51.85±30.58 μm², the mean axonal area was 12.98±11.48 μm², the mean fiber diameter was 7.65±2.74 μm, the mean diameter axonal size was 3.7±1.7 μm, the mean myelin sheath thickness 1.98±0.82 μm and the mean g-ratio was 0.48±0.11. The NM had 12.50% of small, 9.33% of medium and 78.17% of

large myelinated fibers. The MN presented 21.08% of fibers with a diameter lower than 5μm, 77.05% of fibers with a diameter between 5-12 μm and 1.90% of fibers with a diameter higher than 12 μm. The right hemifaces showed lower values ($p<0.05$) compared to left sides for axonal area (11.10±8.58 μm *vs*. 15.08±13.75 μm), axonal diameter (3.46±1.48 μm *vs*. 3.96±1.88 μm) and g-ratio (0.45±0.10 *vs*. 0.51±0.11). The myelin sheath thickness was higher on the right side (2.09±0.84 μm *vs*. 1.85±0.77 μm, $p<0.05$). The results showed similar values in the comparison between the sides to area and nerve fiber diameter ($p>0.05$). **Conclusions**: The data obtained in this study contribute to the identification of a localization region of the masseteric nerve for surgical access and provide microscopic morphometric data to guide masseteric-facial anastomosis procedures in surgical corrections of facial mime musculature paralysis.

Keywords: Masseteric nerve; masseteric artery; macroscopic morphometry; microscopy morphometry.

1. INTRODUÇÃO

O Sistema Nervoso Periférico (SNP) é constituído por 12 pares de nervos cranianos, 31 pares de nervos espinais e gânglios nervosos associados. Os nervos espinais geralmente associam-se entre si formando plexos nervosos (cervical, braquial, lombar, sacral e coccígeo) dando origem aos nervos periféricos. Os nervos cranianos são em ordem de emergência encefálica aparente se são denominados como nervo (I) olfatório, (II) óptico, (III) oculomotor, (IV) troclear, (V) trigêmeo, (VI) abducente, (VII) facial, (VIII) vestibulococlear, (IX) glossofaríngeo, (X) vago, (XI) acessório e (XII) hipoglosso. Funcionalmente os nervos podem ser puramente sensitivos, puramente motores ou mistos (Heimer, 1994).

Estruturalmente, um nervo é formado por fibras nervosas envoltas por uma camada de tecido conjuntivo, o epineuro. As fibras podem estar organizadas em fascículos nervosos, tendo o perineuro como estrutura limitante, separando um fascículo do outro. Nervos podem não apresentar distribuição em forma de fascículos, sendo considerados monofascicular. A camada de tecido conjuntivo que individualiza uma fibra da outra é chamada de endoneuro (Purves et al., 2014).

As fibras nervosas que compõem um nervo são prolongamentos axonais de neurônios motores somáticos (cujo corpo celular está localizado na medula espinal ou em núcleos do tronco encefálico), sensoriais (cujo corpo celular está em gânglios sensitivos) e motores viscerais (cujos corpos celulares estão no SNC e em gânglios viscerais). A bainha de mielina, estrutura lipoproteica depositada ao redor de axônios permite a condução saltatória, rápida e eficaz no sistema nervoso dos vertebrados. As células que constroem a mielina são os oligodendrócitos no SNC e as células de Schwann no SNP (Graça, 1988). As fibras nervosas podem ser mielínicas, em que

encontramos axônios de diferentes calibres envoltos por várias camadas de mielina e amielínicas, as quais são caracterizadas por axônios de pequeno calibre envolvidos por uma única camada de mielina no SNP e nenhuma camada de mielina no SNC (Jotz et al., 2017).

O diâmetro das fibras nervosas e a presença da bainha de mielina são medidas importantes para caracterizar o aspecto funcional do nervo determinando a velocidade de condução do potencial de ação (Bear et al., 2002). As fibras nervosas periféricas podem ser classificadas em A (fibras grandes e mielinizadas dos nervos mistos), B (médias e melinizadas dos nervos motores) e C (pequenas e amielínicas dos nervos mistos). As fibras A podem ser subdivididas em Aα (diâmetro de 13-20 μm e velocidade de condução de 80-120m/s), Aβ (6 a 12 μm e velocidade de condução de 35 a 75m/s), Aγ (diâmetro de 2 a 8 μm e velocidade de condução de 15 a 30 m/s), Aδ (diâmetro de 1 a 5 μm e velocidade de condução de 5 a 30 m/s). As fibras Aα e Aβ apresentam bainha de mielina espessa e as maiores velocidades de condução do impulso nervoso. As fibras Aγ também são mielinizadas e apresentam velocidade de condução moderada. As fibras Aδ são menores e possuem pequeno envoltório mielínico. As fibras B são mielinizadas e possuem diâmetro de 1 a 5 μm e velocidade de condução do impulso de 3 a 15 m/s. As fibras C (diâmetro de 0.2-1.5um e velocidade de condução de 0.5 a 2 m/s) não possuem envoltório mielínico, sendo designadas amielínicas e possuem a menor velocidade de condução do impulso nervoso (Parent, 1996; Purves, 2004; Manzano et al, 2008).

Nos neurônios somatossensoriais, as fibras Aα estão relacionadas à propriocepção dos músculos esqueléticos, as Aβ estão relacionadas com vibração, propriocepção e tato fino, as Aδ com dor e temperatura e as fibras C com temperatura, dor e prurido. As fibras Aα sensoriais também podem ser classificadas como tipo I,

sendo divididas em Ia (fuso muscular) e Ib (órgão tendinoso de Golgi). As fibras Aβ também podem ser classificadas como tipo II (fuso muscular). As fibras Aδ também podem ser classificadas como tipo III. Já as fibras C também podem ser classificadas como tipo IV. Com relação às fibras motoras somáticas, as fibras Aα inervam fibras musculares extrafusais, as Aγ são fibras musculares intrafusais e as Aβ são mais inespecíficas, inervando tanto fibras musculares extrafusais, quanto intrafusais. Com relação as fibras nervosas motoras viscerais, as do tipo B são fibras pré-ganglionares e as do tipo C são fibras pós-ganglionares do sistema nervoso autônomo (Bear et al., 2002; Purves, 2004; Manzano et al, 2008).

O nervo facial (VII par craniano) é um nervo misto e é responsável pela inervação motora dos músculos da mímica facial, músculo estilo-hióideo, ventre posterior do digástrico, músculo estapédio, além de ser o responsável pela sensação de paladar dos dois terços anteriores da língua, como também atua com função parassimpática nas glândulas submandibulares, sublinguais e lacrimais. A função do nervo facial (NF) é crucial não somente para a comunicação, mas também para os principais movimentos faciais como fechamento da boca e dos olhos (Brenner & Schoeller, 1998).

A paralisia do nervo facial é uma enfermidade que acomete 30 a cada 100.000 habitantes mundialmente (Cha et al., 2008). Apresenta-se de forma uni ou bilateral e pode ser central (Corrales et al., 2012), quando acomete o neurônio motor superior, ou periférica (Holtmann et al., 2017), quando há comprometimento do neurônio motor inferior. É caracterizada pela interrupção da inervação motora dos músculos da face que acarreta perda parcial ou total dos movimentos de mímica facial (Domenich Juan et al., 2016). É uma condição debilitante estética, psicológica e funcionalmente (Biglioli et al.,

2017). Há relatos de distúrbios de comunicação, tanto verbal, quanto não verbal como seqüelas desta paralisia (Coombs et al., 2008).

Paralisias faciais podem ser consequência de, por exemplo, remoção de tumores, paralisia de Bell ou trauma (Donnarumma et al., 2014; Yoshioka, 2016; Biglioli et al., 2017). Paralisia de origem congênita como a síndrome de Möbius também podem ocorrer (Cardenas-Mejia & Palafox, 2017). As causas mais comuns de paralisia facial de origem periférica são trauma, infecção, desordens metabólicas, traumatismo ao nascimento, neoplasias, iatrogênicas e idiopáticas (Benecke, 2012). As paralisias de origem central são causadas mais comumente por trauma e derrames (Cattaneo et al., 2010).

O tratamento cirúrgico em pacientes com paralisia do nervo facial se baseia na reinervação da musculatura da mímica da face. É objetivado em casos agudos, crônicos e também durante procedimentos cirúrgicos, imediatamente após a identificação de que o nervo facial fora comprometido (Biglioli et al., 2017; Bianchi et al., 2018). Nesses casos, ramos de nervos cranianos motores podem ser utilizados para reabilitar face paralisada, e para tal podem ser utilizado das seguintes formas: (1) anastomoses diretas ou indiretas de um nervo craniano adjacente ao nervo facial com o nervo facial paralisado (2) inclusão de enxertos nervosos entre o nervo facial paralisado e o nervo facial sadio contralateral e (3) utilização de nervo motor adjacente ao nervo facial para inervar "flap" muscular (Klebuc & Shenaq, 2004).

Ao selecionar um nervo craniano para transferência e anastomose é necessário levar em consideração algumas variáveis: (1) déficit funcional produzido pelo sacrifício do nervo doador, (2) necessidade de interposição de enxerto, (3) sinergismo entre o nervo doador e o nervo facial e sua influência na reeducação motora e (4) topografia nervosa e potencial de neuroreanimação do doador (Klebuc & Shenaq, 2004).

Os nervos motores que geralmente são utilizados para a realização das anastomoses diretas ou indiretas com o nervo facial paralisado, em casos de paralisia facial periférica e central são o nervo hipoglosso (XII par craniano; Manni et al., 2001; Corrales et al., 2012; Socolovsky et al., 2016), nervo espinal acessório (XI par craniano; Placheta et al., 2017; Chuang et al., 2018) e o nervo massetérico, oriundo do ramo mandibular do nervo trigêmeo (V par craniano; Brenner & Schoeller, 1998; Manktelow et al., 2006).

Estudos anatômicos, como o desenvolvido por Fournier et al. (1997), mostram a distribuição do ramo mandibular do nervo trigêmeo (V par craniano) como alternativa de enxertos nervosos comparando-os com as demais possibilidades. Anatomicamente, o nervo trigêmeo é formado por 3 ramos: (V_1) ramo oftálmico, (V_2) ramo maxilar e (V_3) ramo mandibular. Os dois primeiros são puramente sensoriais e o terceiro misto. O nervo oftálmico é responsável pela sensibilidade da cavidade orbital e seu conteúdo. Possui três ramos terminais: nasociliar, frontal e lacrimal. O nervo maxilar inerva as partes moles compreendidas entre a pálpebra inferior, nariz e lábio superior. O nervo mandibular é bastante ramificado, tendo como principais ramos o nervo lingual, que proporciona a sensibilidade geral dos 2/3 anteriores da língua, e o nervo alveolar inferior, que percorre o interior da mandíbula (Moore et al., 2010). A raiz motora do nervo mandibular do trigêmeo dá origem ao nervo temporal profundo posterior, nervo temporal profundo médio, nervo têmporo-bucal e o nervo massetérico (Fournier et al., 1997).

O nervo massetérico (NM) origina-se do ramo mandibular do trigêmeo (V_3) e emerge da fossa infratemporal pela incisura mandibular. Seu trajeto até a face medial do músculo masseter inicia-se no espaço formado pelo arco zigomático, superiormente, e a incisura mandibular, inferiormente. Em um sentido ântero-inferior, aprofunda-se no

músculo masseter, inervando o mesmo (Yoshioka & Tominaga, 2015). Um dos primeiros relatos de caso utilizando o NM na correção de paralisia de nervo facial foi realizado por Bermudez & Nieto (2004) mostrando bons resultados e sem efeitos colaterais.

A localização do NM vem sendo estudada recentemente já que o uso frequente deste nervo em anastomoses nervosas para recuperação em indivíduos com paralisia de nervo facial vem crescendo (Manktelow et al., 2006; Bianchi et al., 2011; Hontonilla & Cabello, 2016, Owusu et al., 2016; Socolovsky et al., 2016; Biglioli et al., 2017; Cardenas-Mejia & Palafox, 2017; Biachi et al., 2018). Pontos anatômicos superficiais como trago e arco zigomático são utilizados como coordenadas de localização do nervo massetérico (Borschel et al., 2012; Cheng et al., 2013; Poddar et al., 2017; Angspatt & Pannanusorn, 2018). Entretanto, alguns autores preferem utilizar referências anatômicas profundas, como articulação temporo-mandibular, processo coronóide da mandíbula e incisura mandibular (Cotrufo et al., 2011; Collar et al., 2013).Por se tratar de um nervo profundo, pouco usual no estudo da anatomia e de baixa utilização clínica, autores descrevem o mesmo como de difícil acesso nas práticas cirúrgicas (Borschel et al., 2011; Cotrufo et al., 2011; Collar et al., 2013; Cheng et al., 2013).

Acompanhando o NM em seu trajeto está a artéria massetérica (AM) (Suzuki, 1998). Essa artéria origina-se da artéria maxilar interna (AMI), em sua porção pterigóide, e é a principal artéria que irriga o músculo masseter (Isolan et al., 2012). A sua proximidade com o NM e com a incisura mandibular explica por que esse vaso é comumente cortado em procedimentos cirúrgicos na região (Rajab et al., 2009).

Nos últimos anos, o NM vem sendo utilizado em reanimação neural de indivíduos com paralisia facial com excelentes resultados (Brenner & Schoeller, 1998; Borschel et al., 2012; Cheng et al., 2013). É um nervo motor doador com grande

capacidade neuroregenerativa. Tal característica está intimamente relacionada ao número total de fibras nervosas mielinizadas em comparação ao nervo receptor. A proporção ideal é de 2:1 (Coombs et al., 2009). Entretanto, dados morfométricos microscópicos a respeito do nervo massetérico são escassos na literatura. Além disso, pelo fato de haver proximidade cortical entre os comandos faciais e mastigatórios, a adaptação é facilitada, a qual pode restaurar não somente tônus muscular e contratibilidade voluntária, como também a ativação espontânea (Lifchez et al., 2005). Manktelow et al. (2006) também fala da proximidade entre os comandos superiores de mastigação e movimentos faciais.

Análises morfométricas (estereologia) são descritas como uma série de procedimentos que permitem uma descrição quantitativa da estrutura, revelando particularmente diferenças morfológicas mínimas entre forma e função (Schenk el al., 2014). A morfometria do nervo fornece informações relevantes para a avaliação de vários fenômenos, como reparo nervoso, regeneração, implante, transplante, envelhecimento e diferentes neuropatias humanas (Waxman, 1980; Novas et al., 2015). As medidas morfométricas microscópicas usualmente utilizadas são: área de seção transversal, número de fascículos, número de fibras nervosas, área das fibras nervosas, área axonal, diâmetro das fibras nervosas, diâmetro axonal, espessura da bainha de mielina e grau de mielinização (g-ratio) do nervo (Schenk et al., 2014).

É neste contexto que o respectivo trabalho visa descrever a localização anatômica e a morfometria microscópica do nervo massetérico em cadáveres humanos e a sua relação anatômica com a artéria massetérica. Os dados permitirão avaliar o potencial de reanimação deste nervo e contribuir para uma abordagem cirúrgica mais segura do nervo massetérico como recurso para reanimação da musculatura da mímica facial.

2. OBJETIVOS

2.1 Objetivo Geral

Descrever morfometricamente o nervo massetérico em cadáveres humanos e a sua relação anatômica com a artéria massetérica.

2.2 Objetivos Específicos

2.2.1 Manuscrito 1

- Descrever o número de ramos do nervo massetérico que cruzam a incisura mandibular em direção ao músculo masseter;
- Descrever parâmetros morfométricos macroscópicos para a localização do nervo massetérico e da artéria massetérica utilizando o trago e o arco zigomático como pontos anatômicos de referência superficiais;
- Comparar os dados morfométricos macroscópicos do nervo massetérico e da artéria massetérica entre cadáveres de homens e mulheres e também entre hemifaces direita e esquerda;
- Avaliar o potencial de reanimação do nervo massetérico mediante contagem do número total de fibras mielinizadas.

2.2.2 Manuscrito 2

- Descrever parâmetros morfométricos microscópicos do nervo massetérico: área de seção transversal, diâmetro total e número de fascículos do nervo, área média das fibras mielinizadas e dos axônios, diâmetro médio das fibras mielinizadas e dos axônios, espessura de bainha de mielina e grau de mielinização (g-ratio);
- Comparar os dados morfométricos microscópicos do nervo entre hemifaces direita e esquerda dos cadáveres.

3. MANUSCRITOS

3.1 Manuscrito 1:

HUMAN MASSETERIC NERVE: NEUROREANIMATION POTENTIAL AND ITS TOPOGRAPHIC AND MORPHOMETRIC RELATIONS WITH THE MASSETERIC ARTERY

Daniel Prato Schmidt[1,2](✉) Eric Kwame Karikari Darko[3] Taís Malysz[1,4]

[1] Programa de Pós-graduação em Neurociências, Instituto de Ciências Básicas da Saúde (ICBS), Universidade Federal do Rio Grande do Sul (UFRGS), Porto Alegre, RS, Brazil.

[2] Departamento de Morfologia, Centro de Ciências da Saúde (CCS), Universidade Federal de Santa Maria (UFSM), Santa Maria, RS, Brazil.

[3] Graduating in Biomedicine, Universidade Federal do Rio Grande do Sul (UFRGS), Porto Alegre, Brazil.

[4] Departamento de Ciências Morfológicas, Instituto de Ciências Básicas da Saúde (ICBS), Universidade Federal do Rio Grande do Sul (UFRGS), Porto Alegre, RS, Brazil.

(✉) Daniel Prato Schmidt

Rua Sarmento Leite, 500

Zip code: 90035-190

Porto Alegre - RS - Brazil

Phone: (55-51) 33083146

E-mail: dpschmidt@hotmail.com

Running Title: A Morphological Study of the Masseteric Nerve

Abstract:

Introduction: The masseteric nerve (MN) has been used in masseteric-facial anastomoses to correct facial nerve palsy. The aim of this study was evaluate the neuroreanimation potential of the MN and to describe topographic and morphometric relations of this nerve with the masseteric artery (MA). **Material and Methods**: Twenty-four hemifaces were dissected and MN and MA were evidenced. The distance of the MN and the MA from the tragus and the zygomatic arch, also the depth of the MN from zygomatic arch from the point which the main branch of the MN crossed the mandibular notch were measured with digital caliper. A nerve fragment was removed and fixed in 2.5% glutaraldehyde solution, submitted to resin inclusion protocol and cross-sectioned (900 nm). The slices were stained in 1% toluidine blue solution. Images were captured and analyzed with software Zeiss ZenBlue 2.3. The cross-sectional area (CSA), nerve diameter and total number of myelinated fibers were analyzed. Student's t test was used to compare values between men and women and right and left hemifaces ($p<0.05$). **Results**: The NM crossed the mandibular notch with 1 (79.1%), 2 (12.5%) or 3 (8.3%) branches to supply the masseter muscle. In all cadavers the MN crossed the mandibular notch together with the MA and was positioned about 2.17±1.24 mm anterior and 1.78±1.79 mm superior to MA. The mean distance from MN and from MA to the tragus was 33.24±3.1 mm and 31.07±2.80 mm, and to the zygomatic arch was 8.34±2.1 mm and 10.11±2.61 mm, respectively. The right hemifaces showed higher distance from MN to the tragus (34.53±2.86 mm *vs*. 31.96±2.88 mm; $p<0.05$) and also from MA (32.29±2.51 mm *vs*. 29.86±2.62 mm; $p<0.05$). MA was more distant from the zygomatic arch in men (11.67±2.80 mm *vs*. 8.56±1.08 mm, $p<0.05$). The mean depth from MN to the zygomatic arch was 11.32±2.1 mm and was higher in men (12.43±2.21 mm *vs*. 10.22±1.26 mm; $p<0.05$). The main branch of the MN presented 1683±315 nerve fibers, the CSA was 0.30±0.1 mm² and the nerve diameter of was 0.76±0.18 mm, with similar values between sides and genders ($p>0.05$). **Conclusions**: The masseteric nerve showed a powerfull neuroreanimation potential for cases of masseteric-facial nerve anastomoses. This study contributed to identification of a localization region for surgical access to the masseteric nerve in human cadavers and the anatomical relation with the masseteric artery.

Keywords: Masseteric nerve; masseteric artery; macroscopic morphometry; microscopic morphometry.

Introduction:

Paralysis of the facial nerve is a disease that affects 30 per 100.000 population worldwide (Cha et al., 2008). It can occur in one or both sides of the face and may be central (Corrales et al., 2012), when it affects the upper motor neuron, or peripheral (Holtmann et al., 2017), when there is impairment of the inferior motor neuron. It is characterized by the interruption of the motor innervation of the muscles of the face that causes partial or total loss of facial motions (Domenich Juan et al., 2016). It is a debilitating condition aesthetically, psychologically and functionally (Biglioli et al., 2017). There are reports of communication disorders, both verbal and nonverbal as sequelae of this paralysis (Coombs et al., 2008).

Surgical treatment in patients with facial nerve palsy is based on the reinnervation of facial mime musculature. It is objectified in acute, chronic cases and also during surgical procedures, immediately after the identification that the facial nerve was compromised (Biglioli et al., 2017). A surgical alternative involves the use of the masseteric nerve as a nerve graft for facial nerve reconstruction which has been approached with promising results (Brenner & Schoeller, 1998; Manktelow et al., 2006).

The masseteric nerve originates from the mandibular branch of the trigeminal and emerges from the infratemporal fossa through the mandibular notch. Its path to the medial aspect of the masseter muscle begins in the space formed by the zygomatic arch, superiorly, and the mandibular notch, inferiorly. In an anterior and inferior sense, it deepens in the masseter muscle, innervating the same (Yoshioka & Tominaga, 2015). Location indicators of the masseteric nerve, varying between superficial and deep, are addressed in several ways by the literature (Cotrufo et al., 2011; Borschel et al., 2011; Biglioli et al., 2012; Collar et al., 2013; Kaya et al., 2014; Yoshioka & Tominaga,

2015). Because it is a deep nerve, unusual in the study of anatomy and low clinical use, many authors describe it as difficult to access in surgical practices (Borschel et al., 2011; Cotrufo et al., 2011; Collar et al., 2013; Cheng et al., 2013).

The masseteric artery originates from the internal maxillary artery, in its pterygoid portion, and is the main artery that irrigates the masseter muscle (Isolan et al., 2012). It is the arterial vessel responsible for irrigation of the deep portion of the masseter (Suzuki, 1998). It accompanies the masseteric nerve in its path and its proximity to the mandibular notch explains why this vessel is commonly cut in surgical procedures in the region (Rajab et al., 2009). To date, there are few anatomical studies involving the masseteric nerve and the masseteric artery.

In the last decades, the masseteric nerve has been used in neuroreanimation of individuals with facial paralysis with excellent results (Brenner & Schoeller, 1998; Borschel et al., 2012; Cheng et al., 2013). Because it is a deep nerve, unusual in the study of anatomy and low clinical use, many authors describe it as difficult to access in surgical practices (Borschel et al., 2011; Cotrufo et al., 2011; Collar et al. Cheng et al., 2013). It is a nerve motor donor with great neuroregenerative capacity. This feature is closely related to the total number of myelinated nerve fibers compared to the receptor nerve. The ideal ratio is 2:1 (Coombs et al., 2009). However, microscopic morphometric data regarding the masseteric nerve are scarce in the literature and need to be done (Fournier et al., 1997).

It is in this context that the respective study aims to evaluate the reanimation potential of the masseteric nerve in human Caucasian Brazilian cadavers and to describe topographic and morphometric relations of this nerve with the masseteric artery. In addition, this study compared the data between men and women, as well as between the

right and left sides, which implies a safer approach of the same as a resource in surgical treatments for reanimation of the facial mime musculature.

Material and methods:

In this study, 12 formalized cadavers were used, six females and six males, totalizing 24 hemifaces, available from the Human Anatomy Laboratory of the Universidade Federal do Rio Grande do Sul (UFRGS), Brazil. The cadavers were obtained by the Institution through a project of voluntary donation in life. Cadavers that had dissected face or that presented some malformation or pathology in the facial region were excluded from the study. Were included cadavers of routines of practical anatomy classes as well as cadavers stored in a conservative solution with no history of use in the laboratory. Both hemifaces were preserved, with no apparent dissection and no physical evidence of pathologies in the study region. They were perfused with 10% formaldehyde fixative solution through a Modial® Injection Pump. This study was registered and approved by local ethics committees.

Each cadaver was placed on the dissection table in a lateral position, both right and left, under its proper illumination. Through an incision in the pre-auricular region, both upper and lower, the skin was folded posterior-anteriorly, remaining fixed at the eye angle and at the angle of the mouth (Fig. 1A).

The superficial muscular aponeurotic system (SMAS) was exposed and carefully dissected for the visualization of important vascular and neural elements, such as the temporal branch, zygomatic branch and buccal branch of the facial nerve and the transverse facial artery. The dissection began by the upper border of the parotid gland towards the zygomatic arch identified by digital palpation. In this region the facial temporal (frontal) branch could be found and from there the division of the zygomatic-temporal trunk. This was used to locate the zygomatic branch of the facial nerve. Through dissection in the anterior portion of the parotid gland the facial buccal branch nerve was found. All branches were dissected to the proximity of the target muscles of

each nerve. The transverse facial artery was identified between the zygomatic and buccal branches of the facial nerve and was dissected to its origin from the superficial temporal artery.

After the individualization of these structures, the masseter muscle was exposed with its proximal fixation evidenced by the cleaning and exposure of the zygomatic arch. The proximal fixation of the masseter muscle was undone, in a region of approximately 2 cm, and deepening dissection, the masseteric nerve and the masseteric artery were visualized emerging from the infratemporal fossa crossing the mandibular notch distributing deeply to the masseter muscle in a anterior and inferior direction.

Branches of the masseteric nerve that crossed the mandibular notch directed towards the deep portion of the masseter muscle were counted. Branches of the masseteric nerve directed to the surface portion of the masseter muscle that did not cross the mandibular notch were not counted.

Macroscopic morphometric data such as horizontal distance from the MN and from the MA to the tragus [MN-tragus (D) and MA-tragus (D'), respectively] and vertical distance from the MN and from MA to the inferior margin of the zygomatic arch aligned over the midpoint of the orbitomeatal line [MN-ZA (d) and MA-ZA (d'), respectively]. The portion of the zygomatic arch used to take the measurements was the inferior margin of the zygomatic arch aligned over the midpoint of the orbitomeatal line (Fig. 1B). The data were collected using a digital caliper (Vonder® 150 mm). The difference between both horizontal distances (D1= D-D') and vertical distances (D2= d'-d) were also calculated (Fig 1C, 1D). Photographic record of the dissected region was performed with digital camera. Measurements were taken in the portion of the MN and of the MA immediately at the point of the emergence from the infratemporal fossa

through the mandibular notch. In the case of the MN emitting collateral branches was considered only the main branch for the measurements.

A 3 mm fragment of the main branch of the masseteric nerve was collected from the portion where the nerve transpose the mandibular notch, placed in 2.5% glutaraldehyde fixative solution (Sigma Chemicals Co) and kept under refrigeration until processing. The histological protocol chosen was inclusion in resin (Durcupan, ACM-Fluka, Buchs, Switzerland). The samples were washed with 0.1M phosphate buffer in three washes of 30 minutes each. Subsequently they were post-fixed with 1% osmium tetroxide (Sigma Chemicals Co) for 60 minutes. Again, they were washed with 0.1 M phosphate buffer in three sets of 15 minutes each. They were then dehydrated with acetone in increasing series of dilution (30%, 50%, 70%, 80%, 90%, 96%) for 10 minutes each and 100% acetone for 20 minutes. The pre-embedding was done in three proportions of resin and acetone (1:3 resin/acetone for 60 minutes, 1:1 resin/acetone overnight and 3:1 resin/acetone for 4 hours). The embedding was made in pure resin molds and vacuum-dried for 24 hours for subsequent oven polymerization for 72-96 hours at 60°C. Through the resin blocks were obtained semithin cross-sections (900 nm) in Leica Ultracut UCT 2.0 ultramicrotome (Merck, Darmstadt, Germany), stained with 1% toluidine blue solution (Malysz et al., 2010). After visualization of the masseteric nerves in the AxioM2 Zeiss, Germany microscope coupled to a digital camera, images of the samples were captured (10X for cross-sectional area and 20X for nerve fiber counting). The microscopic morphometric data analyzed were the total number of myelinated fibers, the diameter and cross-sectional area (CSA) of the nerve.

Descriptive statistical analysis was used to describe averages with standard deviations of the 24 hemifaces of the human cadavers. After the normality of the data were identified, they were analyzed through the Student's t test ($p<0.05$), comparing

morphometric data between right and left hemifaces and between cadavers of men and women. The software used was the Microsoft Office Excel 2010 package.

Results:

The masseteric nerve was originated from the mandibular branch (V_3) from the motor root of the trigeminal nerve (V cranial nerve). The nerve passed over the lateral pterygoid muscle and emerged from the infratemporal fossa. It crossed the mandibular notch and sequentially emitted branches to supply the masseter muscle deeply, accompanied by the masseteric artery. The masseteric nerve traveled anteriorly and inferiorly between the medial and deep portions of the masseter muscle (Fig. 2).

At the region of the mandibular notch the masseteric nerve presented a main branch of greater caliber in all the hemifaces and possible minor branches of the same origin. We found in 19 hemifaces (79.17%) the presence of only one main branch from the masseteric nerve. In three hemifaces (12.5%) we found the presence of one main branch and one thinner branch and in two hemifaces (8.33%) we found the presence of one main branch and two thinner branches. The samples that presented two branches were a female cadaver in both sides and a male cadaver in left hemiface. The samples with the three branching were in a single female cadaver, both in the left and the right hemiface.

In all 24 hemifaces the masseteric nerve was visualized at a position anterior to the MA in relation to the tragus and in 22 cases of the total number of samples (91.66%) the nerve was positioned superior to the artery having the inferior margin of the zygomatic arch aligned over the midpoint of the orbitomeatal line as an anatomical reference (Fig. 3). In only two cases the nerve was located inferiorly to the masseteric artery (8.33%). With this, in most cases the masseteric nerve is found in an anterior and superior anatomical position in relation to the masseteric artery.

The mean distance from the masseteric nerve to the tragus was 33.24±3.10 mm, the mean distance from the masseteric artery to the tragus was 31.07±2.80 mm, the

mean distance from masseteric nerve to the zygomatic arch was 8.34±2.11 mm, the mean distance from masseteric artery to the zygomatic arch was 10.11±2.61 mm. The mean depth from the masseteric nerve to the lower border of the zygomatic arch was 11.32±2.1 mm. The mean difference between the masseteric nerve and masseteric artery distances in relation to the tragus (D1) was 2.17±1.24 mm and the mean difference between masseteric artery and masseteric nerve distances in relation to the zygomatic arch (D2) was 1.78±1.79 mm (n=24). Comparison of the macroscopic morphometric data of male and female genders and right and left hemifaces are shown in Table 1. The distance from the masseteric nerve and the masseteric artery to the tragus was higher in right hemifaces ($p<0.05$). The difference between the horizontal distances (D1) was lower in men ($p<0.05$). The distance of the masseteric artery in relation to the zygomatic arch was higher in men ($p<0.05$). The depth of the masseteric nerve and the distance of the masseteric artery from the zygomatic arch was higher in male cadavers ($p<0.05$).

The masseteric nerve presented mean cross sectional area (CSA) of 0.30±0.1 mm^2 (303040.66±101168.13 μm^2), mean nerve diameter of 0.76±0.18 mm and mean number of 1683±315 myelinated fibers (Fig. 4). The microscopic morphometric data were similar between genders and sides of hemifaces (Table 2).

Discussion:

Most of the authors describe the masseteric nerve of difficult localization (Cotrufo et al., 2011; Poddar et al., 2017), dissection (Fournier et al., 1997; Borschel et al., 2012; Angspatt & Pannanusorn, 2018) and surgical access (Cheng et al., 2013; Collar et al., 2013). However, clinical and surgical studies have proven their efficiency in masseteric-facial anastomoses because of the low morbidity and constant anatomy (Bermudez & Nieto, 2004; Borschel et al., 2009; Cheng et al., 2013; Hontonilla and Marre, 2015; Yoshioka & Tomianaga, 2015; Yoshioka, 2016; Biglioli et al., 2017; Yoshioka, 2017). Total or partial denervation of the masseter muscle does not lead to significant sequelae or loss of masticatory function (Carter & Harkness, 1995; Yoshioka, 2016).

The sample of this study (24 hemifaces) is in agreement with that described in the literature. Collar et al. (2013) used ten cadavers, Poddar et al. (2017) used 24 hemifaces, Angspatt & Pannanusorn (2018) used 28 hemifaces, ranging from a minimum of eight hemifaces by Borschel et al. (2012) and a maximum of 40 hemifaces by Brenner & Schoeller (1998). The samples from the studies were cadaveric, ranging from fresh cadavers (Poddar et al., 2017), frozen cadavers (Collar et al., 2013; Mutori et al., 2014) and formolized cadavers (Fournier et al., 1997; Brenner & Schoeller, 1998; Cotrufo et al., 2011; Borschel et al., 2012; Cheng et al., 2013; Angspatt & Pannanusorn, 2018), as well as the sample in our study.

In our study, we found the masseteric nerve and the masseteric artery emerging from the infratemporal fossa, crossing the mandibular notch. Masseteric nerve originated from the trigeminal mandibular branch (V_3) and masseteric artery from the internal maxillary artery (IMA). Both related to the innervation and irrigation of the masseter muscle. The artery also have participation in the vascularization of the

temporo-mandibular joint (Wysoki et al., 2012; Toure et al., 2018). The masseteric nerve trajectory, described in our results, is in agreement with that reported by Brenner & Schoeller (1998); Huwang et al. (2005), characterizing constancy in the anatomy (Coombs et al., 2009; Hontonilla & Marre, 2015) and masseteric nerve distribution (Fournier et al., 1997).

The masseteric nerve presented a variation of one to three branches in the region of the mandibular notch, always one of them larger them the others (main branch). Brenner & Schoeller (1998) demonstrated in one of the pioneering studies addressing the masseteric nerve, that it can have a variable distribution of one to four branches. These authors found 25% of one branch, 47.2% of two branches, 9% of three branches and 2.8% of four branches. Our data reported the prevalence of 79.17% of one branch, 12.5% of two branches and 8.33% of three branches, showing that there is constancy in the branch pattern of the masseteric nerve. Corroborating with our results, Cotrufo et al. (2011) reported the prevalence of a single branch in 82.35% of the studied hemifaces.

The location of the masseteric nerve has recently been studied as the frequent use of this nerve in anastomoses for recovery in individuals with facial nerve palsy has been increasing (Manktelow et al., 2006; Hontonilla & Cabello, 2016; Owusu et al., 2016; Socolovsky et al., 2016; Biglioli et al., 2017; Cardenas-Mejia & Palafox, 2017; Bianchi et al., 2018; Biglioli et al., 2018). In our study, we used superficial reference anatomical points such as the tragus and the zygomatic arch. These anatomical references were also used by Borschel et al. (2012), Cheng et al. (2013), Poddar et al. (2017) and Angspatt & Pannanusorn (2018). However, some authors preferred to use deep anatomical references, such as temporo-mandibular joint, mandible coronoid process and mandibular notch (Cotrufo et al., 2011; Collar et al., 2013). Anatomical studies that used the tragus and the zygomatic arch as localization indicators for the

masseteric nerve are reliable for the description and standardization of the motor innervation of the masseter muscle for its respective study population. Angspatt & Pannanusorn (2018) used for Thai population, Poddar et al. (2017) used for Indian population and we used to describe a pattern of localization of the masseteric nerve in human Brazilian Caucasian cadavers.

The masseteric artery, also denominated masseteric branch of maxillary artery (MbMA), its originated from the internal maxillary artery by a common trunk (Suwa et al., 1990), it is the main artery that irrigates the masseter muscle (Isolan et al., 2012) and the deep portion of this muscle is irrigated exclusively by the MA (Suzuki, 1989). It passes behind the temporalis tendon and through the mandibular notch to enter the deep surface of the masseter (Won et al., 2012).

In our study, the mean distance from the masseteric nerve to the tragus was 33.24 ± 3.10 mm, the mean distance from the masseteric artery to the tragus was 31.07 ± 2.80 mm, the mean distance from masseteric nerve to the zygomatic arch was 8.34 ± 2.11 mm, the mean distance from masseteric artery to the zygomatic arch was 10.11 ± 2.61 mm. The mean difference between the distances of masseteric nerve and masseteric artery in relation to the tragus (D1) was 2.17 ± 1.24 mm and the mean difference between masseteric nerve and masseteric artery distances in relation to the zygomatic arch (D2) was 1.78 ± 1.79 mm. The mean depth from the masseteric nerve to the inferior margin of the zygomatic arch was 11.32±2.09 mm.

Borschel et al. (2012) studying the anatomy of the masseteric nerve in Caucasian male cadavers reported similar measures, such as 31.60±0.30 mm, 13.30±0.20 mm and 14.80±0.19 mm for the distances of the masseteric nerve to the tragus, to the zygomatic arch and its depth, respectively. Cheng et al. (2013) described 22.90±2.61 mm and 12.22±3.68 mm as the mean of the distances from masseteric nerve to the tragus and the

zygomatic arch, respectively. Angspatt & Pannanusorn (2018), in Thai population, found 37.00±0.4 mm, 8.00±0.2 mm and 11.00±0.2 mm for the same measurements obtained in our study with a lot similarity. We used the inferior margin of the zygomatic arch aligned over the midpoint of the orbitomeatal line for anatomical reference for the measurements. Kaya et al. (2014) and Poddar et al. (2017) termed the midpoint of the orbitomeatal line as "R point". The portion of the main branch of the masseteric nerve that crosses the mandibular notch was chosen to be the target of the measurements.

Our data demonstrated a significant difference in the depth of the masseteric nerve in relation to the inferior border of the zygomatic arch in a segmentation by gender, being superior in men (12.43±2.21 mm vs. 10.22±1.26 mm; $p<0.05$). Corroborating with our study Poddar et al. (2017) reported the same difference in the depth variable. The difference between the horizontal distances (D1) was lower in men, showing that the masseteric nerve and the masseteric artery are closer to each other than women. We also found that was a significant difference in a segmentation by hemiface sides, with the distance of the masseteric nerve to the tragus (34.53±2.86 mm vs. 31.96±2.88 mm, $p<0.05$) and distance of the masseteric artery to the tragus (32.29±2.51 mm vs. 29.86±2.62 mm, $p<0.05$) higher on the right side. In men, the distance from masseteric artery to the zygomatic arch was higher than in women. No other study compared the data in this way, to our knowlegde, since most of the samples were random hemifaces of anatomical collection, which prevented the comparison between hemifaces of the same cadaver. It is in this sense that our study has a strongly positive point, the standardization of the samples that allowed both an analysis of data between genders and sides of hemifaces.

We used the tragus and the zygomatic arch as superficial anatomical reference points for this study because they are concomitant references to the location of the

masseteric nerve and with this we can study the distribution of these elements (masseteric artery and masseteric nerve) with a focus on surgical access of the region in situations of nerve anastomoses for the correction of facial nerve paralysis. This allows us to locate the nerve easier and also minimizes risk of vascular lesions, bleeding and making the surgical procedures of the region less bloody.

Fournier et al. (1997) reported that histological studies on the masseteric nerve are necessary. More than 20 years have passed and this question has changed little. Our study revealed that the main branch of masseteric nerve presented a very evident epineurium involving a complex of myelinated nerve fibers ranging from 1269 to 2315 fibers. Although the existent studies do not report the portion of the masseteric nerve of human cadavers evaluated histologically, Coombs et al. (2009) quantified 1543±292 myelinated fibers, whereas Borschel et al. (2012) found 2775±470 fibers. We found 1683±315 myelinated fibers in our study. These numbers show a powerful neuroreanimation potential that the masseteric nerve possesses, since Coombs et al. (2009) show the occurrence of 100-200 fibers in the zygomatic branch of the facial nerve and 834±285 fibers in the buccal branch of the facial nerve. It exceeds the ratio of 2:1 that Coombs et al. (2009) mentions in his study. The mean diameter was 0.75±0.18 mm, which is in accordance with that proposed by Cotrufo et al. (2011) which refers to 0.6mm diameter as good for masseteric-facial reanimation.

This study is unique when studying Brazilian Caucasian samples, both macroscopically and microscopically, providing a pattern of localization of the masseteric nerve using the tragus and the zygomatic arch as superficial anatomical reference points. Based on this, we were able to identify a region of nerve location, thus facilitating its surgical approach and dissection. We also verified the anatomical constancy and branching pattern. We could also evaluate the potential of

neuroreanimation that the masseteric nerve may have as a donor in anastomoses with the facial nerve in individuals who have paralysis of the mime musculature. This work can be useful anatomically and clinically, and can be used in the development of models of nerve localization, which applied in clinical practice, assist the surgeons in their procedures.

Conclusions:

The main branch of the masseteric nerve has approximately 1638 myelinated fibers which mean that this segment of the masseteric nerve seems to be an excellent donor in cases of surgical procedures like masseteric-facial anastomoses. The nerve was identified approximately 3.3 cm anteriorly of the tragus and 0.8 cm inferiorly to the zygomatic arch. The depth of the nerve in relation to the zygomatic arch was approximately 1.1 cm, being deeper in men. The masseteric nerve and the masseteric artery have an intimate relationship running together through the mandibular notch to the masseter muscle. These structures are closer to each other in men and more distant from the tragus in the right side of the face. The masseteric artery is more distant vertically from the zygomatic arch in men. This study contributed to identification of a localization region for surgical access to the masseteric nerve in human cadavers and the anatomical relation with the masseteric artery.

Conflicts of interest:

The authors have no conflicts of interest to declare.

Acknowledgements:

We wish to thank Silvia Barbosa, Chris Krebs and Maikel Rosa de Oliveira for their help in the preparations of the histological samples.

References:

1. Angspatt, A., & Pannanusorn, C. (2018). The masseteric nerve: An anatomical study in Thai population with an emphasis on its use in facial reanimation. Asian Journal of Surgery, 41(5), 486–489.

2. Bermudez, L., & Nieto, L. (2004). Masseteric-Facial Nerve Anastomosis: Case Report. Journal of Reconstructive Microsurgery, 21(01), 25–30.

3. Bianchi, B., Varazzani, A., Pedrazzi, G., Poddi, V., Ferrari, S., Brevi, B., & Ferri, A. (2018). Masseteric cooptation and crossfacial nerve grafting: Is it still applicable 22 months after the onset of facial palsy? Microsurgery, 1–7.

4. Biglioli, F., Soliman, M., El-Shazly, M., Saadeldeen, W., Abda, E. A., Allevi, F., & Califano, L. (2018). Use of the masseteric nerve to treat segmental midface paresis. British Journal of Oral and Maxillofacial Surgery, 1–8.

5. Biglioli, F., Colombo, V., Rabbiosi, D., Tarabbia, F., Giovanditto, F., Lozza, A., & Mortini, P. (2017). Masseteric–facial nerve neurorrhaphy: results of a case series. Journal of Neurosurgery, 126(1), 312–318.

6. Biglioli, F., Frigerio, A., Colombo, V., Colletti, G., Rabbiosi, D., Mortini, P., & Brusati, R. (2012). Masseteric–facial nerve anastomosis for early facial reanimation. Journal of Cranio-Maxillofacial Surgery, 40(2), 149–155.

7. Borschel, G. H., Kawamura, D. H., Kasukurthi, R., Hunter, D. A., Zuker, R. M., & Woo, A. S. (2012). The motor nerve to the masseter muscle: An anatomic and histomorphometric study to facilitate its use in facial reanimation. Journal of Plastic, Reconstructive & Aesthetic Surgery, 65(3), 363–366.

8. Brenner, E., & Schoeller, T. (1998). Masseteric nerve: A possible donor for facial nerve anastomosis? Clinical Anatomy, 11(6), 396–400.

9. Cardenas-Mejia, A., & Palafox, D. (2018). Facial reanimation surgery in Möbius syndrome: Experience from 76 cases from a tertiary referral hospital in Latin America. Annales de Chirurgie Plastique Esthétique, 63(4), 338–342.

10. Carter., G. M., & Harkness, E. M. (1995). Alterations to Mandibular Form Following Motor Denervation of the Masseter Muscle. An experimental Study in Rat. Journal Anatomy, 186, 541-548.

11. Cha, C. I., Hong, C. K., Park, M. S., & Yeo, S. G. (2008).Comparison of Facial Nerve Paralysis in Adults and Children. Yonsei Medical Journal, 49(5), 725–734.

12. Cheng, A., Audolfsson, T., Rodriguez-Lorenzo, A., Wong, C., & Rozen, S. (2013). A reliable anatomic approach for identification of the masseteric nerve. Journal of Plastic, Reconstructive & Aesthetic Surgery, 66(10), 1438–1440.

13. Collar, R. M., Byrne, P. J., & Boahene, K. D. O. (2013). The Subzygomatic Triangle. Plastic and Reconstructive Surgery, 132(1), 183–188.

14. Coombs, C. J., Ek, E. W., Wu, T., Cleland, H., & Leung, M. K. (2009). Masseteric-facial nerve coaptation – an alternative technique for facial nerve reinnervation. Journal of Plastic, Reconstructive & Aesthetic Surgery, 62(12), 1580–1588.

15. Corrales, C. E., Gurgel, R. K., & Jackler, R. K. (2012). Rehabilitation of Central Facial Paralysis With Hypoglossal-Facial Anastomosis. Otology & Neurotology, 33(8), 1439–1444.

16. Cotrufo, S., Hart, A., Payne, A. P., Sjogren, A., Lorenzo, A., & Morley, S. (2011). Topographic anatomy of the nerve to masseter: An anatomical and clinical study. Journal of Plastic, Reconstructive & Aesthetic Surgery, 64(11), 1424–1429.

17. Doménech Juan, I.,Tornero, J., Cruz Toro, P., Ortiz Laredo, N., Vega Celiz, J., Junyent, J., & MañosPujol, M. (2014). Cirugía reparadora de la parálisis facial mediante colgajo libre microvascularizado de músculo gracilis. Acta Otorrinolaringológica Española, 65(2), 69–75.

18. Fournier, H.-D., Denis, F., Papon, X., Hentati, N., & Mercier, P. (1997). An anatomical study of the motor distribution of the mandibular nerve for a masseteric-facial anastomosis to restore facial function. Surgical and Radiologic Anatomy, 19(4), 241–244.

19. Holtmann, L. C., Eckstein, A., Stähr, K., Xing, M., Lang, S., & Mattheis, S. (2017). Outcome of a graduated minimally invasive facial reanimation in patients with facial paralysis. European Archives of Oto-Rhino-Laryngology, 274(8), 3241–3249.

20. Hontanilla, B., & Cabello, A. (2016). Spontaneity of smile after facial paralysis rehabilitation when using a non-facial donor nerve. Journal of Cranio-Maxillofacial Surgery, 44(9), 1305–1309.

21. Hontanilla, B., & Marre, D. (2015). Masseteric-facial nerve transposition for reanimation of the smile in incomplete facial paralysis. British Journal of Oral and Maxillofacial Surgery, 53(10), 943–948.

22. Hwang, K., Kim, Y. J., Chung, I. H., & Song, Y. B. (2005). Course of the Masseteric Nerve in Masseter Muscle. Journal of Craniofacial Surgery, 16(2), 197-200.

23. Isolan GR, Pereira AH, Pires de Aguiar PH, Antunes ACM, Mousquer JP, Pierobon M R. Anatomia microcirúrgica da artéria carótida externa: um estudo estereoscópico. J Vasc Bras 2012; 11(1):3–11.

24. Kaya, B., Apaydin, N., Loukas, M., & Tubbs, R. S. (2014). The topographic anatomy of the masseteric nerve: A cadaveric study with an emphasis on the effective zone of botulinum toxin A injections in masseter. Journal of Plastic, Reconstructive & Aesthetic Surgery, 67(12), 1663–1668.

25. Malysz, T., Ilha, J., Nascimento, P. S., De Angelis, K., Schaan, B. D., & Achaval, M. (2010). Beneficial effects of treadmill training in experimental diabetic nerve regeneration. Clinics, 65(12), 1329-1337.

26. Manktelow, R. T., Tomat, L. R., Zuker, R. M., & Chang, M. (2006). Smile Reconstruction in Adults with Free Muscle Transfer Innervated by the Masseter Motor Nerve: Effectiveness and Cerebral Adaptation. Plastic and Reconstructive Surgery, 118(4), 885–899.

27. Moturi, S. (2014). To Evaluate the Feasibility of Neurotisation of Facial Nerve Branches with Ipsilateral Masseteric Nerve: An Anatomic Study. Journal of Clinical and Diagnostic Research, 8(4), 4–7.

28. Owusu, J. A., Truong, L., & Kim, J. C. (2016). Facial Nerve Reconstruction With Concurrent Masseteric Nerve Transfer and Cable Grafting. JAMA Facial Plastic Surgery, 18(5), 335–339.

29. Poddar, R., Bhattacharya, A., Sinha, & I. Ghosal, A. K. (2017). An Anatomical study for localisation of Zygomatic branch of Facial nerve and Masseteric nerve - An aid to nerve coaptation for facial reanimation surgery: A cadaver based study in Eastern India. Indian Journal of Plastic Surgery, 50(1), 74-78.

30. Rajab BM, Sarraf AA, Abubaker AO, Laskin DM.Masseteric Artery: Anatomic Location and Relationship to the Temporomandibular Joint Area. Journal of Oral and Maxillofacial Surgery 2009; 67(2):369–371.

31. Socolovsky, M., Martins, R. S., Di Masi, G., Bonilla, G., & Siqueira, M. (2016). Treatment of complete facial palsy in adults: comparative study between direct hemihypoglossal-facial neurorrhaphy, hemihipoglossal-facial neurorrhaphy with grafts, and masseter to facial nerve transfer. Acta Neurochirurgica, 158(5), 945–957.

32. Suwa F, Takemura A, Ehara Y, Takeda N, Masu M. On the arteriamaxillaris which passes medial to the pterygoideuslateralis muscle of the Japonese patterns of origin of the inferior alveolar, the masseteric and the posterior temporal arteries. Okajimas Folia AnatJpn 1990; 67(5):303–308.

33. Suzuki T. Arterial supply to the masseter muscle in the rat. Kaibogakuzasshi 1989; 64(1):8–17.

34. Toure G. Arterial Vascularization of the Mandibular Condyle and Fractures of the Condyle. Plastic and Reconstructive Surgery 2018; 141(5):718e–725e.

35. Won SY, Choi DY, Kwak HH, KimST, Kim HJ, Hu KS. Topography of the arteries supplying the masseter muscle: Using dissection and Sihler's method. Clinical Anatomy 2011;25(3):308–313.

36. Wysocki J, Reymond J, Krasucki K. Vascularization of the mandibular condylar head with respect to intracapsular fractures of mandible. Journal of Cranio-Maxillofacial Surgery 2012; 40(2):112–115.

37. Yoshioka, N. (2017). Differential Reanimation of the Midface and Lower Face Using the Masseteric and Hypoglossal Nerves for Facial Paralysis. Operative Neurosurgery, 15(2), 174–178.

38. Yoshioka, N. (2016). Masseter Atrophication after Masseteric Nerve Transfer. Is It Negligible? Plastic and Reconstructive Surgery - Global Open, 4(4), e692.

39. Yoshioka, N. (2016). Masseteric Nerve as “Baby Sitter” Procedure in Incomplete Facial Paralysis.Plastic and Reconstructive Surgery - Global Open, 4(4), e669.

40. Yoshioka, N., & Tominaga, S. (2015). Masseteric nerve transfer for short-term facial paralysis following skull base surgery. Journal of Plastic, Reconstructive & Aesthetic Surgery, 68(6), 764–770.

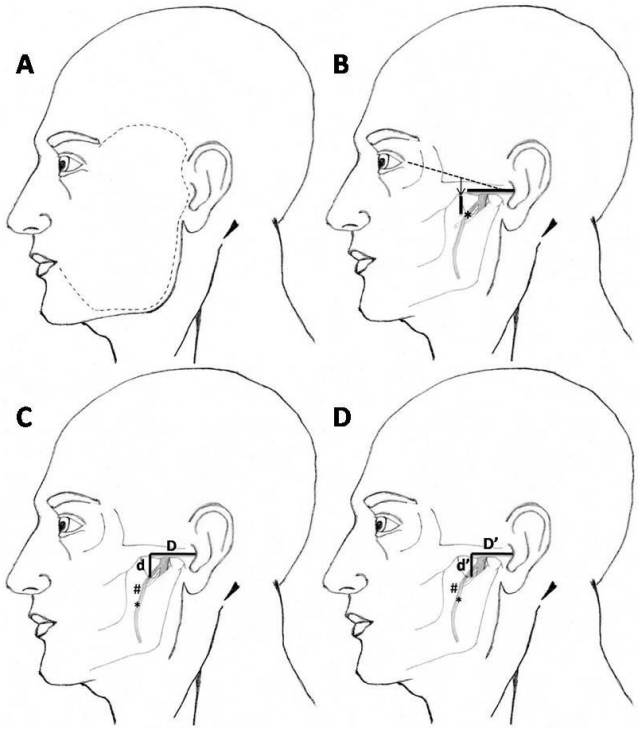

Figure 1:Illustrative schematization of a left human hemiface showing skin incision and macroscopic morphometric parameters measured. (A) Pre-auricular incision extended anteriorly and inferiorly to eye angle and mouth angle. (B) Location measurements of the main branch of the masseteric nerve at the point where the nerve transverses the mandibular notch (*). Orbitomeatal line (----); alignment with the inferior border of the zygomatic arch (arrow). (C) D - distance from masseteric nerve to the tragus; d - distance from masseteric nerve to the inferior margin of the zygomatic arch aligned over the midpoint of the orbitomeatal line. (D) D' - distance from masseteric artery to the tragus; d' - distance from masseteric artery to the inferior margin of the zygomatic arch aligned over the midpoint of the orbitomeatal line. * - Masseteric nerve (MN); # - Masseteric artery (MA).

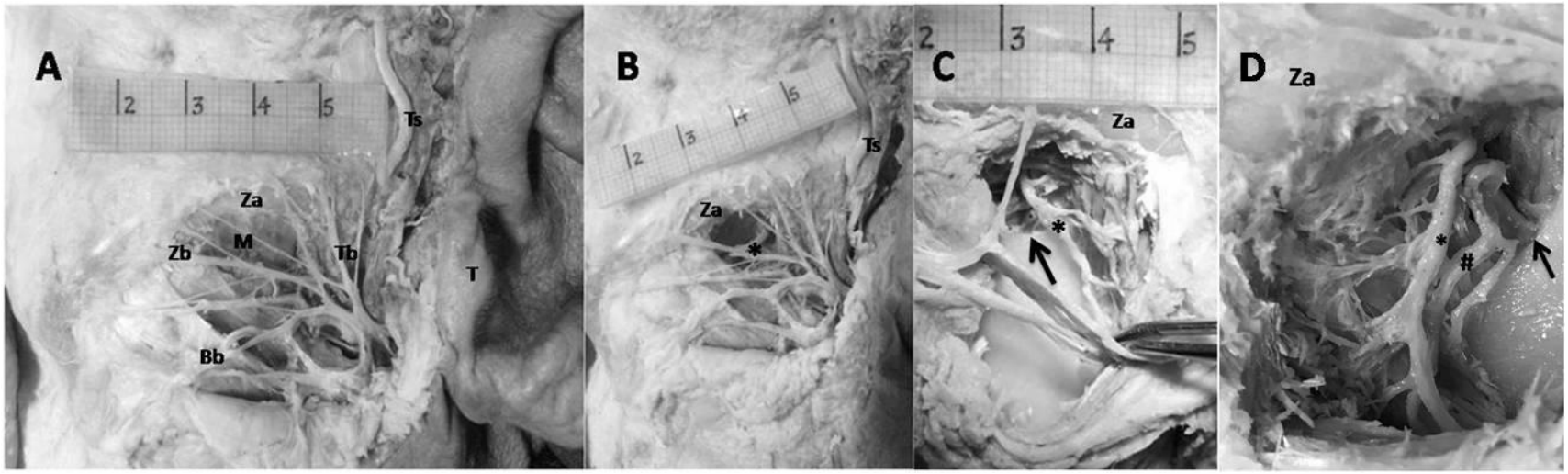

Figure 2: Lateral view of dissected human cadaveric hemifaces. (A) Surface dissection of a left hemiface with the superficial muscular aponeurotic system (SMAS) dissected showing branches of the facial nerve (Tb, Zb, Bb) and temporal superficial vessels. (B) Deep dissection of a left hemiface. Observe the removal of the proximal fixation of the masseter muscle from the inferior border of the zygomatic arch. Masseteric nerve (*) in depth. (C) Deep dissection of a right hemiface. Observe the masseteric nerve (*) emerging from the infratemporal fossa crossing the mandibular notch and traversing a path between the layers of the masseter muscle and issuing branches. (D) Deep dissection of a cadaveric human left hemiface. Observe the masseteric nerve (*) and the masseteric artery (#) emerging from the infratemporal fossa crossing the mandibular notch and traversing a path between the layers of the masseter muscle and issuing branches. Ts: superficial temporal artery and vein, Tb: temporal branch, Zb: zygomatic branch, Bb: buccal branch, Za: zygomatic arch, T: tragus, M: masseter muscle, ↑ mandibular notch, scale (cm).

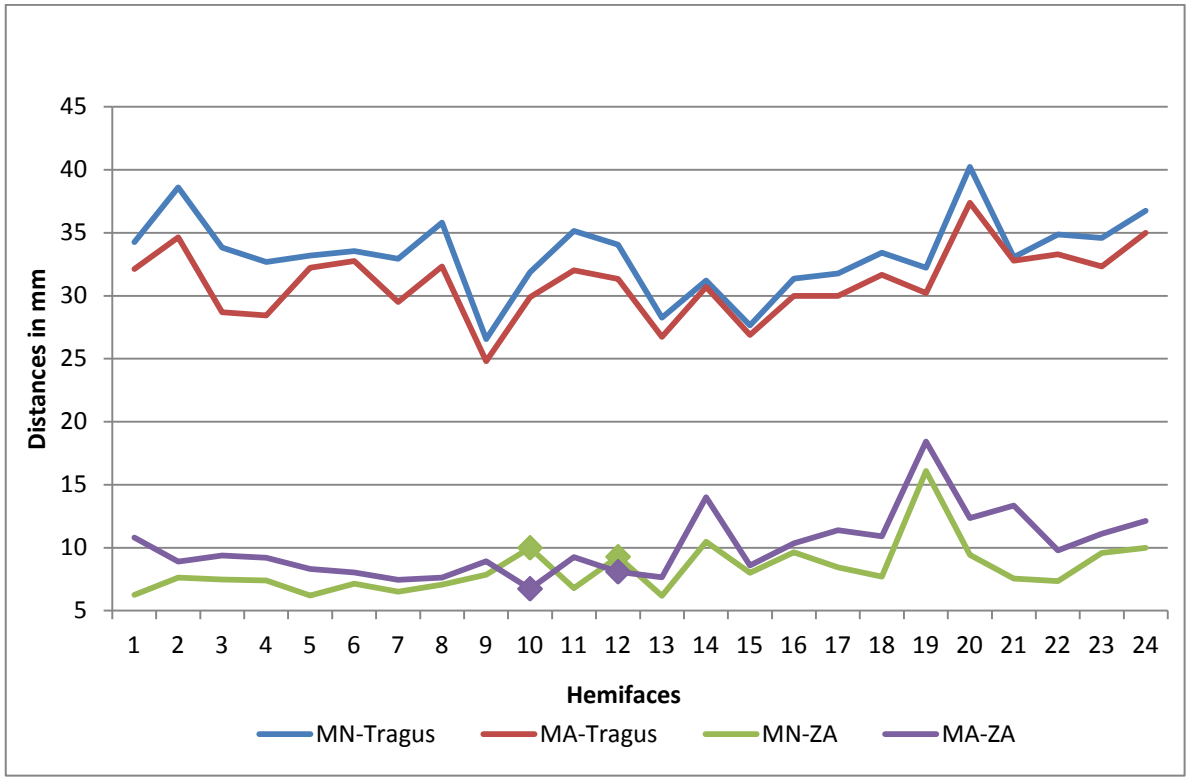

Figure 3: Graphic showing the relationship of the MN and the MA from different distances (from the tragus and from the inferior margin of the zygomatic arch). Note that the MN was found always further from the tragus compared to the MA. In most cases (n=22) the MN was closer to the zygomatic arch rather than the MA, indicating that the nerve is positioned superiorly to the artery. In two cases there were inversions of this pattern as marked on the bottom lines of the graphic. MN-Tragus: horizontal distance from the MN to the tragus; MA-Tragus: horizontal distance from the MA to the tragus; MN-ZA: vertical distance from the MN to the inferior margin of the zygomatic arch aligned over the midpoint of the orbitomeatal line; MA-ZA: vertical distance from the MA to the inferior margin of the zygomatic arch aligned over the midpoint of the orbitomeatal line.

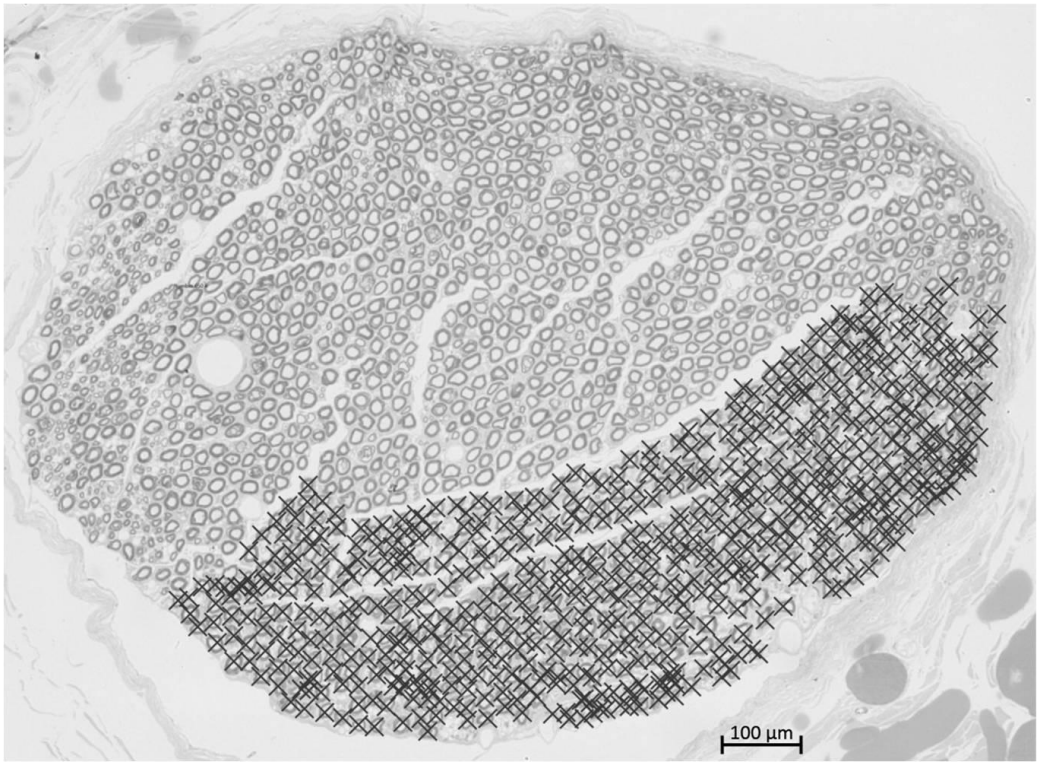

Figure 4: Digitized image of semithin cross-section obtained from the portion of the main branch of the masseteric nerve that crosses the mandibular notch collected from human formolized cadavers. Application of stereological method for nerve fiber counting whrere "x" was marked over each fiber counted manually. Toluidine blue stained. (A) 20 X, Bar=100 µm.

Table1: Macroscopic morphometric data of the masseteric nerve and masseteric artery showing gender and sides of hemiface segmentation.

Hemiface	MN-Tragus	MA-Tragus	D1	MN-ZA	MA-ZA	D2	Depth of MN
Male	32.95±3.46	31.42±3.06	1.53±0.74*	9.21±2.52	11.67±2.80*	2.46±1.41	12.43±2.21*
Female	33.54±2.81	30.73±2.61	2.81±1.33	7.47±1.15	8.56±1.08	1.09±1.92	10.22±1.26
Right	34.53±2.86#	32.29±2.51#	2.24±1.20	8.59±1.31	9.84±2.18	1.25±1.94	11.03±2.09
Left	31.96±2.88	29.86±2.62	2.10±1.32	8.08±2.73	10.39±3.06	2.30±1.52	11.62±2.14

Data expressed as mean ± standard deviation (mm). MN - Masseteric nerve; MA - Masseteric artery; ZA - Zygomatic arch; D1 - Difference between the horizontal distances of MN and MA; D2 - Difference between the vertical distances of MN and MA; #$p<0.05$ *vs*. left hemiface; *$p<0.05$ *vs*. female cadaver.

Table 2: Microscopic morphometric data of the masseteric nerve showing gender segmentation and sides of hemiface.

Hemiface	Cross-sectional area (μm²)	Myelinated fibers number	Diameter (μm)
Male	335928.59±97889.09	1630.33±340.41	789.34±189.40
Female	270152.74±97253.65	1703.25±327.07	720.24±169.18
Right	286533.21±118158.29	1488.80±138.16	733.26±197.34
Left	319548.12±82731.59	1845.50±337.29	776.32±164.77

Data expressed as mean ± standard deviation.

3.2 Manuscrito 2

MICROSCOPIC MORPHOMETRY AND DEGREE OF MYELINATION (G-RATIO) IN HUMAN MASSETERIC NERVE

Daniel Prato Schmidt[1,2](✉) Felipe Bastos[3] Taís Malysz[1,4]

[1] Programa de Pós-graduação em Neurociências, Instituto de Ciências Básicas da Saúde (ICBS), Universidade Federal do Rio Grande do Sul (UFRGS), Porto Alegre, RS, Brazil.

[2] Departamento de Morfologia, Centro de Ciências da Saúde (CCS), Universidade Federal de Santa Maria (UFSM), Santa Maria, RS, Brazil.

[3] Graduating in Physiotheraphy, Universidade Federal do Rio Grande do Sul (UFRGS), Porto Alegre, Brazil.

4 Departamento de Ciências Morfológicas, Instituto de Ciências Básicas da Saúde (ICBS), Universidade Federal do Rio Grande do Sul (UFRGS), Porto Alegre, RS, Brazil.

(✉) Daniel Prato Schmidt

Rua Sarmento Leite, 500

Zip code:90035-190

Porto Alegre - RS - Brazil

Phone: (55-51) 33083146

E-mail: dpschmidt@hotmail.com

Running Title: Morphometry and g-ratio of the masseteric nerve

Abstract:

Introduction: Morphometric analyzes are powerful tools for deeply describing a cranial or peripheral nerve. **Objectives**: The aim of this study is to morphometrically describe the masseteric nerve in human cadavers. **Material and Methods**: Twelve MN from human cadavers were dissected and one fragment was removed and fixed in 2.5% glutaraldehyde solution, submitted to resin inclusion protocol and cross-sectioned (900 nm). The slices were stained in 1% toluidine blue solution. Five images of each nerve were captured and analyzed with software Zeiss ZenBlue 2. The area of the nerve fiber, axon area, fiber diameter, axonal diameter, myelin thickness and myelination degree (g-ratio) were calculated with means and standard deviation. Student's t test was used to compare the variables between right and left sides of the faces ($p<0.05$).**Results**: The mean fiber and axonal area were 51.85±30.58 μm² and 12.98±11.48 μm², respectively. The mean fiber and axonal diameter were 7.65±2.74 μm and 3.7±1.7 μm. The mean myelin thickness was 1.98±0.82μm and the mean g-ratio was 0.48±0.11. The NM had 12.50% of small, 9.33% of medium and 78.17% of large myelinated fibers. The MN presented 21.08% of fibers with a diameter lower than 5μm, 77.05% of fibers with a diameter between 5-12 μm and 1.90% of fibers with a diameter higher than 12 μm. The right hemifaces showed lower values ($p<0.05$) compared to left sides for axonal area (11.10±8.58 μm *vs*. 15.08±13.75 μm), axonal diameter (3.46±1.48 μm *vs*. 3.96±1.88 μm) and g-ratio (0.45±0.10 *vs*. 0.51±0.11). The myelin sheath thickness was higher on the right side (2.09±0.84 μm *vs*. 1.85±0.77 μm, $p<0.05$). The results showed similar values in the comparison between the sides to area and nerve fiber diameter ($p>0.05$).**Conclusions**: The masseteric nerve is a monofascicular nerve with higher perceptual of large fibers with thick myelin sheath, with diameter most of all between 5-12 μm and high degree of myelination.

Keywords: Morphometry; masseteric nerve; g-ratio.

Introduction:

Morphometric analyzes are powerful tools for deeply describing a cranial or peripheral nerve. It is described as a series of procedures that allows a quantitative description of structure, particularly revealing minimal morphological differences between form and function. Nerve morphometry is known to produce relevant information for the evaluation of several phenomena, such as nerve repair, regeneration, implant, transplant, aging, and different human neuropathies (Waxman, 1980; Novas et al., 2015). Those are complementary data to an anatomical study that describes path and topography. By associating macroscopy with microscopy, we can well describe an anatomical structure in its complexity. The microscopic morphometric measures usually used are: cross-sectional area, number of fascicles, number of nerve fibers, nerve fiber area, axon area, nerve fiber diameter, axonal diameter, myelin sheath thickness, and degree of myelination (g-ratio) of the nerve (Schenk et al., 2014).

The relationship between Schwann cells and axon directly influences the conduction velocity of the nerve fiber as follows: an increase in axonal diameter stimulates thickening of its myelin sheath, which is associated with elongation of the internodal segment and a consequent increase in the saltatory conduction velocity of the nerve impulse (Thomas & Ochoa, 1984). Myelination is a unique cellular process that can have a dramatic impact on the structure and physiology of an axon and its tissue surroundings (Chomiak & Hu, 2009). Myelin plays a key role increasing speed of action potential conduction along axons and improving neurological function (West et al., 2016).

The conduction velocity of an action potential through the membrane depends on the diameter of nerve fiber and degree of myelination (Bolat et al., 2017). This velocity is proportional to fiber diameter, and there is an optimum ratio of myelin

thickness to fiber diameter for maximal conduction velocity (Ikeda et al., 2012). It has been shown that there is a range of values between axon size and myelin thickness for optimal efficiency in healthy tissue (Chomiak & Hu, 2009).

The degree of myelination (g-ratio) describes the relationship between axon size and myelin thickness, and deviations in the g-ratio are thought to be involved in abnormal development and disease (West et al., 2015). Rushton (1951) was the first to present the relationship between axonal diameter and the thickness of its myelin sheath as a g-ratio and considered a g-ratio value of 0.6 to be theoretical optimal for the conduction velocity of nerve impulses. The g-ratio, calculated by the ratio of the inner axonal diameter to the total outer diameter (Ugrenovic et al., 2015), can be useful to the evaluation of the fiber morphology during peripheral nerve regeneration and in studies in the area of microsurgery (Páfaro et al., 2018).

To date, there are none morphometric studies involving the masseteric nerve. Therefore the aim of this study is to morphometrically describe and calculate the g-ratio of the masseteric nerve in human cadavers by introducing this data in the literature and compare the data between right and left side of the cadavers.

Material and methods:

In this study, 6 formalized cadavers (age 54-88) were used, five females and one male, totalizing 12 hemifaces, available from the Human Anatomy Laboratory of the Universidade Federal do Rio Grande do Sul (UFRGS), Brazil. The cadavers were obtained by the Institution through a project of voluntary donation in life. Cadavers that had dissected face or that presented some malformation or pathology in the facial region were excluded from the study. Were included cadavers of routines of practical anatomy classes as well as cadavers stored in a conservative solution with no history of use in the laboratory. Both hemifaces were preserved, with no apparent dissection and no physical evidence of pathologies in the study region. They were perfused with 10% formaldehyde fixative solution through a Modial® Injection Pump. This study was registered and approved by local ethics committees.

Each cadaver was placed on the dissection table in a lateral position, both right and left, under its proper illumination. Through an incision in the pre-auricular region, both upper and lower, the skin was folded posterior-anteriorly, remaining fixed at the eye angle and at the angle of the mouth.

The superficial muscular aponeurotic system (SMAS) was exposed and carefully dissected for the visualization of important vascular and neural elements, such as the temporal branch, zygomatic branch and buccal branch of the facial nerve and the transverse artery of the face. The dissection began by the upper border of the parotid gland towards the zygomatic arch identified by digital palpation. In this region the facial temporal (frontal) branch could be found and from there the division of the zygomatic-temporal trunk. This was used to locate the zygomatic branch of the facial nerve. Through dissection in the anterior portion of the parotid gland the facial buccal branch nerve was found. All branches were dissected to the proximity of the target muscles of

each nerve. The transverse facial artery was identified between the zygomatic and buccal branches of the facial nerve and was dissected to its origin from the superficial temporal artery.

After the individualization of these structures, the masseter muscle was exposed with its proximal fixation evidenced by the cleaning and exposure of the zygomatic arch. The proximal fixation of the masseter muscle was undone, in a region of approximately 2 cm, and deepening dissection, the masseteric nerve and the masseteric artery were visualized emerging from the infratemporal fossa crossing the mandibular notch distributing deeply to the masseter muscle in an anterior and inferior direction.

A 3 mm fragment from the main branch of the masseteric nerve was collected from the portion where the nerve transpose the mandibular notch, placed in 2.5% glutaraldehyde fixative solution (Sigma Chemicals Co) and kept under refrigeration until processing. The histological protocol chosen was inclusion in resin (Durcupan, ACM-Fluka, Buchs, Switzerland). The samples were washed with 0.1M phosphate buffer in three washes of 30 minutes each. Subsequently they were post-fixed with 1% osmium tetroxide (Sigma Chemicals Co) for 60 minutes. Again, they were washed with 0.1 M phosphate buffer in three sets of 15 minutes each. They were then dehydrated with acetone in increasing series of dilution (30%, 50%, 70%, 80%, 90%, 96%) for 10 minutes each and 100% acetone for 20 minutes. The pre-embedding was done in three proportions of resin and acetone (1:3 resin/acetone for 60 minutes, 1:1 resin/acetone overnight and 3:1 resin/acetone for 4 hours). The embedding was made in pure resin molds and vacuum-dried for 24 hours for subsequent oven polymerization for 72-96 hours at 60°C. Through the resin blocks were obtained semithin cross-sections (900 nm) in Leica Ultracut UCT 2.0 ultramicrotome (Merck, Darmstadt, Germany), stained with 1% toluidine blue solution (Malysz et al., 2010). After visualization of the masseteric

nerves in the AxioM2 Zeiss, Germany microscope coupled to a digital camera, five images of the samples (one central e four peripheral) were captured (100X for morphometry). The microscopic morphometric data analyzed were the mean area of the myelinated fibers, the mean area of axons, the mean diameter of the nerve fiber, the mean diameter of the axon, mean myelin thickness and the degree of myelination (g-ratio). A region of interest (ROI) with 1015.12 μm² was drawn in each image. All fibers inside and those that contact with the upper and left lateral margin of the ROI were analyzed. A mean of 45±12 myelinated nerve fibers were analyzed by nerve in a total of 536 nerve fibers analyzed. The total area analyzed for each nerve was 5075.60 μm². The software used to analyze the samples was Zeiss ZenBlue 2.3 eddition (Fig. 1B).

To estimate the axonal diameter, the axonal area of each individual fiber was measured and the value obtained was converted to the diameter of a circle with equivalent area by the formula $2\sqrt{(A/\pi)}$. The fiber diameter (axon + myelin sheath) was calculated by the same formula. To estimate the myelin thickness we subtracted the estimated diameter of the axon (d) from that of the whole nerve fiber (D) by the formula (D-d)/2 modified from Ramkumar et al. (2015). We organized and analyzed the myelinated nerve fibers based on their fiber area, classifying them into small (<10 μm²), medium (10-20 μm²) and large (>20 μm²) (Sharma et al., 2009). The g-ratio for each of the analyzed nerve fibers was then calculated from the ratio of the inner axonal diameter (d) to the total outer diameter (D) according to the formula g = d/D (Ugrenovic et al., 2015).

Descriptive statistical analysis was used to describe averages with standard deviations of the 12 hemifaces of the human cadavers. After the normality of the data were identified, they were analyzed through the Student's T test ($P<0.05$), comparing

morphometric data between right and left hemifaces of the cadavers. The software used was the Microsoft Office Excel 2010 package.

Results:

The masseteric nerve appears as a monofascicular nerve with myelinated fibers well distributed, ensheathed by thin connective tissue that sent incomplete septa carrying branches of small blood vessels to the central portion (Fig.1A). Analyzing the histological aspect of samples we could see the prevalence of large nerve fibers but also the presence of thinly myelinated fibers most common in the peripheral part of the nerve close to the epineurium.

Fiber area of myelinated fibers. The fiber area of myelinated fibers of the masseteric nerve ranged from 1.75 μm² to 137.78 μm². The mean fiber area was 51.85±30.58 μm². Overall, the masseteric nerve had 12.5% small, 9.33% medium and 78.17% large myelinated fibers (Fig.2A).

Diameter of myelinated fibers. The diameter of myelinated fibers of the masseteric nerve ranged from 1.49 μm to 13.25 μm. The mean fiber diameter was 7.65 ± 2.74 μm. Overall, the masseteric nerve had 21.08% of fibers with diameter lower than 5 μm, 77.05% of fibers with diameter between 5-12 μm and 1.90% fibers with diameter higher than 12 μm (Fig.2B).

Axonal area of myelinated fibers. The axonal area of myelinated fibers of the masseteric nerve ranged from 0.28 μm² to 71.66 μm². The mean axonal area was 12.98±11.48 μm².

Axonal diameter of myelinated fibers. The axonal diameter of myelinated fibers of the masseteric nerve ranged from 0.59 μm to 9.55 μm. The mean axonal diameter was 3.7±1.7μm.

Myelin thickness. The myelin thickness of myelinated fibers of the masseteric nerve ranged from 0.41 μm to 4.30 μm. The mean myelin thickness was 1.98±0.82 μm.

Degree of myelination (g-ratio) of myelinated fibers. The g-ratio of myelinated fibers of the masseteric nerve ranged from 0.2 to 0.81. The mean g-ratio was 0.48±0.11.The scatter plots illustrate the distribution of the g-ratio related to the diameter of the nerve fiber (Fig.3).

Comparing the analyzed data between right and left sides of the hemifaces, significant difference were found in axonal area, axonal diameter and g-ratio, which were lower on the right side than the left side. Only the myelin thickness was higher in the right side compared to the left hemiface ($p<0.05$). The fiber area and the fiber diameter of the myelinated nerve fibers do not showed significant difference ($p>0.05$) (Table 1).

Discussion:

The cross-sections of the nerves revealed various shapes, the most common being oval and circular for the masseteric nerve, although on many occasions they were irregular due to their thin epineurium. These data are in agreement with the data of Ramkumar et al. (2015) that described the same observations in human trochlear and abducens nerves.

The masseteric nerve is classically described as a motor nerve since its fibers are directed to the masseter muscle (Cotrufo et al., 2011). Our study revealed that the masseteric nerve is a monofascicular nerve. This structural arrangement was also described by Borschel et al. (2012) in human masseteric nerve. However, Moturi et al. (2014) identified the presence of seven to ten nervous fascicles in the motor nerve to masseter. This may be justified by methodological differences in histological processing and interpretation.

The mean fiber diameter of the masseteric nerve was 7.65±2.74 μm, with 21.08% of fibers with diameter lower than 5 μm, 77.05% of fibers with diameter between 5-12 μm and 1.90% fibers with diameter higher than 12 μm. These fibers diameters were used to make functional associations according to the Erlanger and Gasser classification (Parent, 1996). In this classification, motor Aγ fibers, intended to supply intrafusal muscle fibers, have diameter lower than 5 μm, Aβ fibers, to both intrafusal and extrafusal muscle fibers, have diameter between 5-12 μm and motor Aα fibers, to extrafusal muscle fibers, have diameter higher than 12 μm. Thus, it is possible that most of the myelinated nerve fibers (77.05%) of the human masseteric nerve are destined to innervate intrafusal and extrafusal muscle fibers. Furthermore, based on this analysis, other fibers of this nerve would be directed exclusively to intrafusal (21.08%) and extrafusal (1.9%) muscle fibers.

According to Kerns (1980), small myelinated nerve fibers can be used to supply intrafusal muscle fibers and slow extrafusal muscle fibers. Considering that the masseter muscle has around 50% of slow muscle fibers (Rowlerson et al., 2005), it is possible that a great part of myelinated nerve fibers with a diameter of 5-12um are directed to supply such muscle fibers.

According to that used in studies with cranial nerves such as trochlear and abducens nerve we divided the fibers of the masseteric nerve into three groups (small fibers <10 μm², medium fibers 10-20 μm² and large fibers >20 μm²) (Ramkumar et al., 2015). We found 12.50% of small, 9.33% of medium and 78.17% of large fibers based on the total fiber area. Ramkumar et al. (2015) reported the presence of 8.83% of small, 30.39% of medium and 60.78% of large fibers in abducens nerve. They also reported 17.95%, 35.9% and 46.15% for the same groups in trochlear nerve. By converting the areas of nerve fibers in diameter by the formula $2\sqrt{(A/\pi)}$, we could see that small and medium nerve fibers would include fibers with diameter up to 5 μm and large fibers would include fibers larger than 5 μm. These differences may be explained by the fact that are different group of muscles with differentiated functions, being the ocular musculature responsible for more refined movements than the masticatory muscles.

The cranial nerves may present a greater number of proprioceptive fibers (Abo-El-Enene, 1978) to the muscle, which may justifies having a larger sum of small and medium fibers than those described in our study. These small and medium fibers would have an estimated diameter of up to 5 μm, which is compatible with Aγ fibers. The large fibers are compatible with the estimated diameter of Aβ (5-12 mm) and Aα (> 12 mm) fibers, which supply both intrafusal and extrafusal fibers.

The mean axonal area, from cadavers with age 54 to 88, in our study was 12.98±11.48 μm². These data are in accordance with reported by Sharma et al. (2009) which described the mean of 9.71±0.71 μm² in oculomotor nerve for people above 71 years old. Ramkumar et al. (2015) showed 19.45±2.64 μm² of axonal area in trochlear nerve and 23.72±6.01 μm² in abducens nerve for people above 60 years old. These studies showed no difference in axonal area in between groups of different ages.

The mean myelin thickness, from cadavers with age 54 to 88, in our study was 1.98±0.82 μm. Sharma et al.(2009) reported the mean of 2.06±0.33 μm in oculomotor nerve for people above 71 years old. Ramkumar et al. (2015) showed 2.48±0.39 μm in trochlear nerve and 2.90±0.51 μm for abducens nerve for people above 60 years old. These studies compared with younger categories and the myelin thickness seems to have increased with age. That is why the myelin sheath is thicker in our study. Myelin thickness apparently increases with age, probably due to addition of newer lamellae (Peters, 2002). Hence, it can be suggested that the irregular myelin profiles and connective tissue changes in the older age could be due to altered nerve growth factor (NGF) or similar other factors that need further confirmation using specific biochemical markers.

The mean g-ratio in our study was 0.48 ±0.11, varying from 0.2 to 0.81. De Campos et al. (2015) reported in recurrent laryngeal nerve the g-ratio varying from 0.61±0.01 to 0.68±0.05. Páfaro et al. (2018) for hypoglossal nerve compared the left (0.90±0.1) with the right (0.88±0.1) side and saw that there are no statistically significant difference between then. For peripheral nerves, like sciatic nerve, Ugrenovic et al. (2015) demonstrated that the g-ratio varied from 0.7 to 0.9 in 60-80 years old people.

Observing the scatter plots we could verify that in the individual less than 60 years of age, the g-ratio was in the optimal zone, while in the older individuals the g-ratio was less than 0.6, being between 0.37 and 0.59. This refers to the presence of a thicker myelin sheath and demonstrates that the masseteric nerve presents a high degree of myelination in the studied sample. This may be a normal pattern of the masseteric nerve in humans given the importance of rapid stimuli to the masticatory musculature. However, there are no data in the literature for comparison.

Thomas & Ochoa (1984) further cited that g-ratio values lower than 0.4 indicate the presence of degenerated nerve fibers with abnormal thickening of the myelin sheath, whereas values higher than 0.7 indicate either regenerated fibers with thinner myelin sheath, or demyelinated nerve fibers. This may be the explanation why in some samples the g-ratio was less than 0.6. Furthermore, time after death and time up to the fixation of the cadaver may interfere. We do not have a medical history of the cadavers used in our study to eliminate the possibilities of some associated neuropathy that may interfere with the reported g-ratio.

Comparing the analyzed data between right and left sides of the hemifaces we found significant difference being the axonal area, axonal diameter and g-ratio lower on the right side than the left side. The myelin thickness was higher in the right side compared to the left hemiface. The fiber area and the fiber diameter of the myelinated nerve fibers do not showed significant difference. In order to verify the chewing preferences of the most people, Zamanlu et al. (2012) showed that 47.36% of the subjects appear to prefer chewing with the right side and only 10.53% to 26.32% prefer chewing using the left side of the mouth, demonstrating that is a tenable assumption that most people prefer to chew with the right side. This functional consideration may

explain why the myelin sheath is thicker and the g-ratio value is lower on the right side of the face. However, further studies are needed to elucidate these observations.

Due to the heterogeneity of our sample we could not analyze statistically whether there are significant differences between men and women or compare the g-ratio between different ages. However, the data are important due to the total lack of information about this about the masseteric nerve in the literature. Future studies may corroborate this data and establish better relationships between different genders and age groups.

Conclusions:

The masseteric nerve is a monofascicular nerve with large fibers but also a large number of small axons with high myelin thickness and high degree of myelination. The masseteric nerve presented 51.85±30.58 μm² of nerve fiber area, 12.98±11.48 μm² of axon area, a mean myelin sheath thickness of 1.98±0.82μm and a mean g-ratio of 0.48±0.11. Our results provide values for future studies aimed at further elucidating the functional and morphological patterns of the masseteric nerve.

Conflicts of interest:

The authors have no conflicts of interest to declare.

References:

1. Waxman, S. G. 1980. Determinants of conduction velocity in myelinated nerve fibers. Muscle Nerve 3:141–150.

2. Novas, R. B., Fazan, V. P. S., & Felipe, J. C. (2015). A New Method for Automated Identification and Morphometry of Myelinated Fibers Through Light Microscopy Image Analysis. Journal of Digital Imaging, 29(1), 63–72.

3. Schenk, H. C., Haastert-Talini, K., Jungnickel, J., Grothe, C., Meyer, H., Rehage, J., & Tipold, A. (2014). Morphometric Parameters of Peripheral Nerves in Calves Correlated with Conduction Velocity. Journal of Veterinary Internal Medicine, 28(2), 646–655.

4. Thomas, P. K, & Ochoa J. (1984). Microscopic anatomy of the peripheral nervous system. In: Dyck PJ, Thomas PK (eds) Peripheral neurophathy, 2nd ed. Saunders, London, 39–91.

5. Chomiak, T., & Hu, B. (2009). What Is the Optimal Value of the g-Ratio for Myelinated Fibers in the Rat CNS? A Theoretical Approach. PLoS ONE, 4(11), e7754.

6. West, K. L., Kelm, N. D., Carson, R. P., & Does, M. D. (2016). A revised model for estimating g-ratio from MRI. NeuroImage, 125, 1155–1158.

7. Bolat, D., Yıldız, D., Bahar, S., Yürüker, S., Kaymaz, F., Ilgın, C., & Sabancı, S. (2017). A comparative study of oculomotor, trochlear and abducens nerves in Arabian foals. Biotechnic & Histochemistry, 92(2), 149–156.

8. Ikeda, M., & Oka, Y. (2012). The relationship between nerve conduction velocity and fiber morphology during peripheral nerve regeneration. Brain and Behavior, 2(4), 382–390.

9. Rushton, W.A. (1951). A theory of the effects of fibre size in medullated nerve. J Physiol 115(1):101–122.

10. Ugrenović, S., Jovanović, I., Vasović, L., Kundalić, B., Čukuranović, R., & Stefanović, V. (2015). Morphometric analysis of the diameter and g-ratio of the myelinated nerve fibers of the human sciatic nerve during the aging process. Anatomical Science International, 91(3), 238–245.

11. Páfaro, J. N., Goulart, G. R., Silveira, C. H., Cella, P. A. M., Malysz, T., Jotz, G. P., & Campos, D. (2018). Degree of Myelination (g-ratio) of the Human Hypoglossal Nerve. Journal of Morphological Sciences, 35(01), 25–27.

12. Malysz, T., Ilha, J., Nascimento, P. S., De Angelis, K., Schaan, B. D., & Achaval, M. (2010).Beneficial effects of treadmill training in experimental diabetic nerve regeneration. Clinics, 65(12), 1329–1337.

13. Ramkumar, M., Sharma, S., G. Jacob, T., N. Bhardwaj, D., C. Nag, T., & Sankar Roy, T. (2015). The Human Trochlear and Abducens Nerves at Different Ages - a Morphometric Study. Aging and Disease, 6(1), 6–16.

14. Cotrufo, S., Hart, A., Payne, A. P., Sjogren, A., Lorenzo, A., & Morley, S. (2011). Topographic anatomy of the nerve to masseter: An anatomical and clinical study. Journal of Plastic, Reconstructive & Aesthetic Surgery, 64(11), 1424–1429.

15. Borschel, G. H., Kawamura, D. H., Kasukurthi, R., Hunter, D. A., Zuker, R. M., & Woo, A. S. (2012). The motor nerve to the masseter muscle: An anatomic and histomorphometric study to facilitate its use in facial reanimation. Journal of Plastic, Reconstructive & Aesthetic Surgery, 65(3), 363–366.

16. Moturi, S. (2014). To Evaluate the Feasibility of Neurotisation of Facial Nerve Branches with IpsilateralMasseteric Nerve: An Anatomic Study. Journal of Clinical and Diagnostic Research, 8(4), 4–7.

17. Parent, A. Carpenter's human neuroanatomy. 9thEd. Baltimore: Williams & Wilkins, 1996.

18. Kerns, J. M. (1980) Postnatal differentiation of the rat thochlear nerve. Journal of Comparative Neurology, 189, 291–306.

19. Rowlerson, A., Raoul, G., Daniel, Y., Close, J., Maurage, C.-A., Ferri, J., & Sciote, J. J. (2005). Fiber-type differences in masseter muscle associated with different facial morphologies. American Journal of Orthodontics and Dentofacial Orthopedics, 127(1), 37–46.

20. Abo-El-Enene, M. A. (1978). Proprioceptive afferent fibers in the cranial nerves III, IV and VI. Cells Tissues Organs, 101(1), 62–65.

21. Sharma, S., Ray, B., Bhardwaj, D., Dwivedi, A. K., & Roy, T. S. (2009). Age changes in the human oculomotor nerve – A stereological study. Annals of Anatomy - Anatomischer Anzeiger, 191(3), 260–266.

22. Peters, G. B. 3rd, Bakri, S. J., & Krohel, G. B. (2002). Cause and Prognosis of nontraumatic sixth nerve palsies in young adults. Ophthalmology, 109: 1925-1928.

23. De Campos, D., Xavier, L. L., Goulart, G. R., Thomaz, L. D. G. R., Malysz, T., & Jotz, G. P. (2015). Similarities in the surface area/volume ratio in the fibers of the

recurrent laryngeal nerve can explain the symmetry in the vocal fold mobility? Medical Hypotheses, 85(6), 989–991.

24. Zamanlu, M., Khamnei, S., SalariLak, S., Oskoee, S. S., Shakouri, S. K., Houshyar, Y. & Salekzamani, Y. (2012). Chewing side preference in the first and all mastication cycles for hard and soft morsels. Int J Clin Exp Med, 5(4): 326-331.

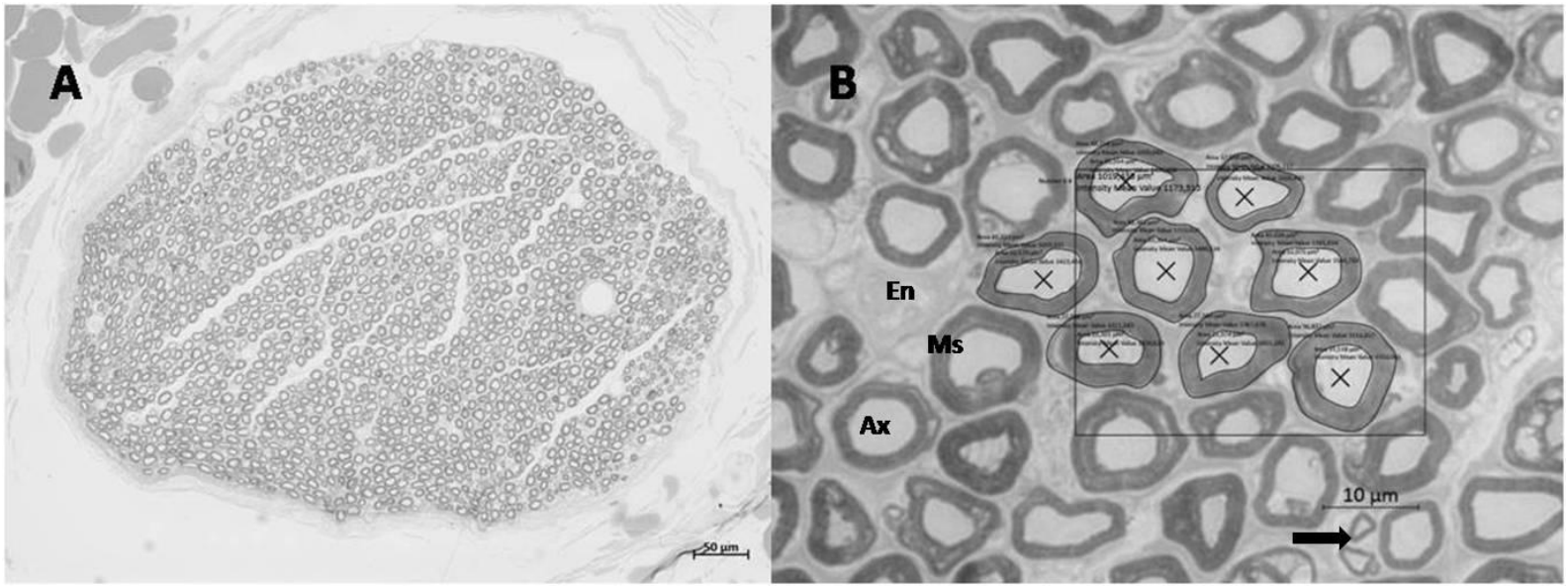

Figure 1: Digitized images of semithin cross-sections obtained from masseteric nerve in human formolized cadavers. (A) Note the monofascicular aspect of the masseteric nerve. (B) Application of stereological method. Region of interest (ROI) of 1015.12 µm². Fibers inside the ROI and any fibers the made contact with the superior and the left margins of the ROI were included in the analyses (X). Observe the presence os small nerve fibers (arrow). Toluidine blue stained. (A) 20 X, Bar = 50 µm. (B) 100 X, Bar = 10 µm. Ax: axon; Ms: myelin sheath; En: endoneurium.

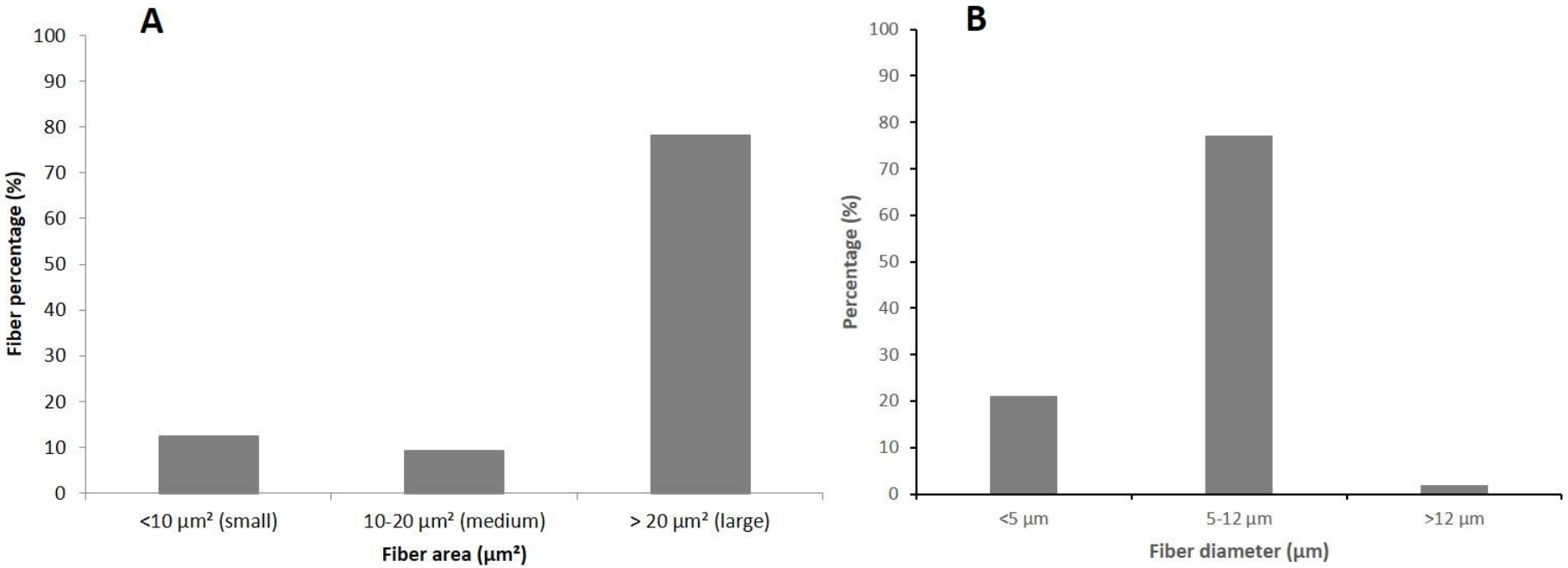

Figure 2: Histogram of myelinated fiber in masseteric nerve of the human cadavers. (A) Fiber percentage (%) in relation with the total fiber area. (B) Fiber percentage (%) based in the fiber diameter. In "A" 12.50% are small, 9.33% medium and 78.17% large fibers. In "B" 21.08% with diameter of lower than 5 µm,77.05% with diameter of 5-12 µm and 1.9% with diameter higher than 12 µm.

Table 1: Microscopic morphometric data of the masseteric nerve.

Hemiface	Fiber area (μm²)	Axonal area (μm²)	Fiber diameter (μm)	Axonal diameter (μm)	G-ratio	Myelin thickness (μm)
Right	51.44±29.50	11.10±8.58*	7.63±2.70	3.46±1.48*	0.45±0.10*	2.09±0.84*
Left	52.30±31.80	15.08±13.75	7.67±2.79	3.96±1.88	0.51±0.11	1.85±0.77

Data expressed as mean ± standard deviation. G-ratio: degree of myelination. * $p<0.05$ *vs.* left hemiface.

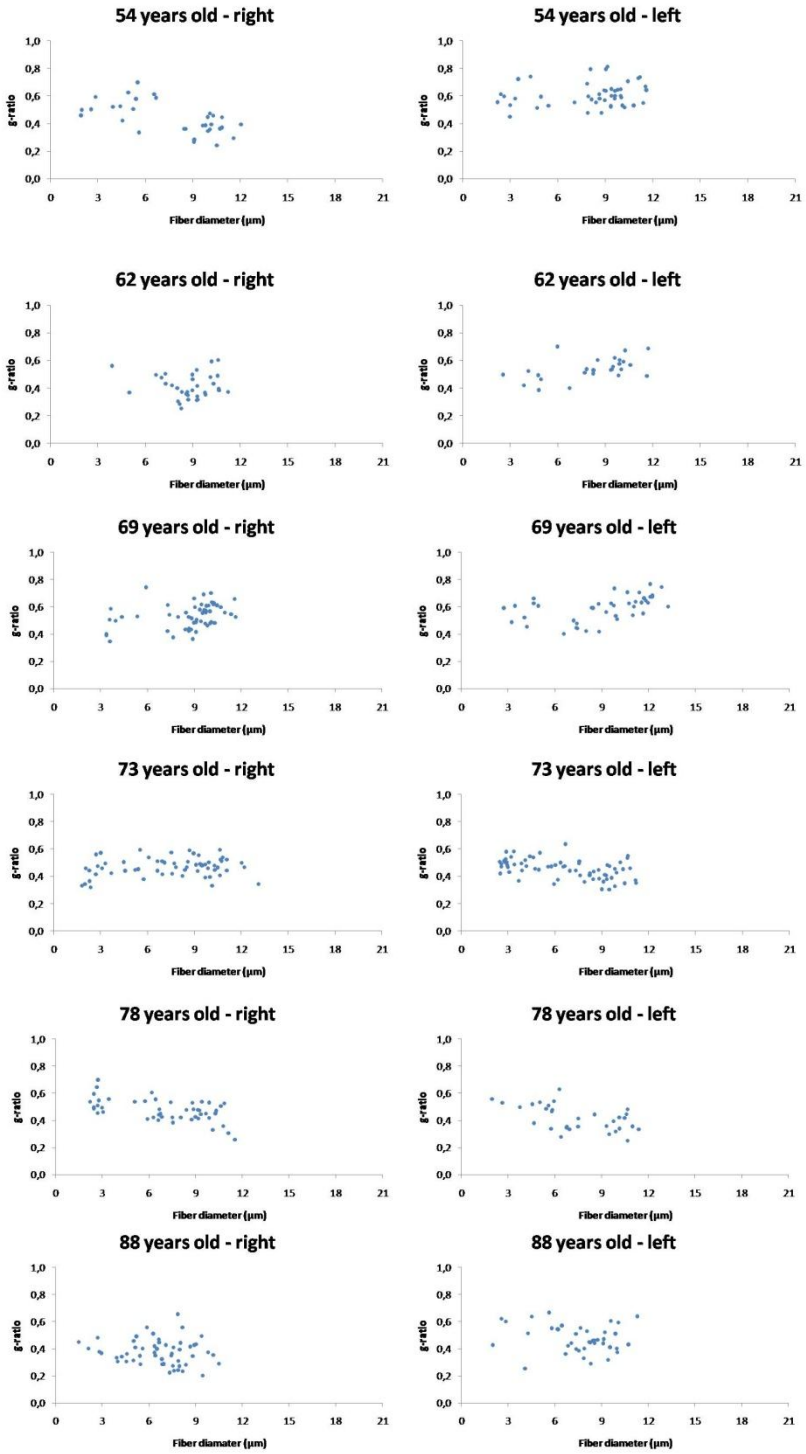

Figure 3: Scatter plots of the g-ratio and diameter of the nerve fibers of all evaluated cases organized by age.

4. DISCUSSÃO GERAL

O nervo massetérico é descrito como de difícil localização (Cotrufo et al., 2011; Poddar et al., 2017), dissecação (Fournier et al., 1997; Borschel et al., 2012; Angspatt & Pannanusorn, 2018) e acesso cirúrgico (Cheng et al., 2013; Collar et al., 2013). Entretanto, estudos clínicos comprovaram sua eficiência em anastomoses masseterico-faciais devido à baixa morbidade e anatomia constante do nervo (Bermudez & Nieto, 2004; Borschel et al., 2009; Cheng et al., 2013; Hontonilla & Marre, 2015; Yoshioka & Tomianaga, 2015; Yoshioka, 2016; Biglioli et al., 2017; Yoshioka, 2017).

A topografia do nervo massetérico, descrita em nossos resultados, está de acordo com a relatada por Brenner & Schoeller (1998); Huwang et al. (2005), caracterizando constância na anatomia (Coombs et al., 2009; Hontonilla & Marre, 2015). Em nosso estudo, encontramos o nervo massetérico (NM) e a artéria massetérica (AM) emergindo da fossa infratemporal, cruzando a incisura mandibular. O NM originou-se do ramo mandibular trigeminal (V_3) e a AM da artéria maxilar interna (AMI). Ambos relacionados à inervação e irrigação do músculo masseter.

O nervo massetérico apresentou variação de um a três ramos na porção relacionada à incisura mandibular. Quando a ramificação é superior a um ramo, sempre um ramo apresentava maior calibre que os demais, sendo considerado assim, por nós, como o ramo principal do nervo massetérico. Brenner & Schoeller (1998) demonstraram que o nervo pode ter uma distribuição variável de um a quatro ramos. Esse autor encontrou 25% de um ramo, 47,2% de dois ramos, 9% de três ramos e 2,8% de quatro ramos. Nossos dados relataram a prevalência de 79,17% de um ramo, 12,5% de dois ramos e 8,33% de três ramos. Corroborando com nossos resultados Cotrufo et al. (2011) relatam a prevalência de um único ramo em 82,35% das hemifaces estudadas.

Para a localização do NM utilizamos pontos anatômicos de referência superficiais, como o trago e o arco zigomático. Essas referências também foram utilizadas por Borschel et al. (2012), Cheng et al. (2013), Poddar et al. (2017) e Angspatt & Pannanusorn (2018). No entanto, alguns autores preferiram utilizar referências profundas, como a articulação temporo-mandibular (ATM), o processo coronóide da mandíbula e a incisura mandibular (Cotrufo et al., 2011; Collar et al., 2013).

Em nosso estudo, a distância média do NM ao trago foi de 33,24±3,10 mm e ao arco zigomático foi de 8,34±2,11 mm. A profundidade média do nervo massetérico em relação a borda inferior do arco zigomático foi de 11,32±2,09 mm. Borschel et al. (2012) relataram medidas semelhantes, como 3,16±0,30 cm, 1,33±0,20 cm e 1,48±0,19 cm para as mesmas variáveis. Cheng et al. (2013) descreveram 22,90±2,61 mm e 12,22±3,68 mm como médias das distâncias do NM ao trago e ao arco zigomático, respectivamente. Angspatt & Pannanusorn (2018) obtiveram 3,7±0,4 cm, 0,8±0,2 cm e 1,1±0,2 cm para as mesmas medidas, respectivamente, e com muita semelhança com o nosso estudo.

Nossos dados demonstraram uma diferença significativa na profundidade do NM em relação à borda inferior do arco zigomático em uma segmentação por gênero, sendo superior em homens (12,43±2,21 mm vs. 10,22±1,26 mm; $p<0,05$). Corroborando com o nosso estudo, Poddar et al. (2017) relatou a mesma diferença na variável profundidade.Acredita-se que essa diferença na profundidade do nervo massetérico seja devido a maior hipertrofia das fibras musculares do músculo masseter em indivíduos do sexo masculino. Constatamos também que houve diferença significativa na segmentação por lados da hemiface, com a distância do nervo massetérico ao trago superior do lado direito (34,53±2,86 mm vs. 31,96±2,88 mm, $p<0,05$). Nenhum outro

autor comparou os dados desta forma, uma vez que a maioria das amostras utilizadas para seus trabalhos foram hemifaces aleatórias de acervo anatômico, o que impediu a comparação entre as hemifaces do mesmo cadáver.

No nosso estudo a AM acompanhou o NM e se mostrou superior e anterior a este na maioria dos casos. A distância média da AM ao trago foi de 31,07±2,80 mm e ao o arco zigomático foi 10,11±2,61 mm. A diferença média entre as distâncias de NM e AM em relação ao trago (D1) foi de 2,17±1,24 mm e a diferença média entre as distâncias NM e AM em relação ao arco zigomático (D2) foi de 1,78±1,79 mm. Nos homens, a distância da AM ao arco zigomático foi maior que nas mulheres ($p<0,05$). Também foi demonstrado que o NM e a AM são mais distantes entre si nas mulheres, na porção que cruza a incisura mandibular, do que nos homens ($p<0,05$). Além disso, o NM e a AM estavam mais distantes do trago na hemiface direita do que na esquerda ($p<0,05$). Não há dados na literatura para comparar esses resultados.

Fournier et al. (1997) relataram que estudos histológicos no NM são necessários devido à falta de informações na literatura. Nosso estudo revelou que o NM é um nervo monofascicular o que está de acordo com Borschel et al. (2012). O nervo apresentou um epineuro evidente envolvendo um complexo de fibras nervosas mielinizadas variando de 1269 a 2315 fibras. Coombs et al. (2009) quantificaram 1543±292 fibras mielinizadas, enquanto Borschel et al. (2012) encontraram 2775±470 fibras. Encontramos em média 1683±315 fibras mielinizadas em nosso estudo. Esses números mostram o poderoso potencial de neuroreanimação que o NM possui, uma vez que Coombs et al. (2009) mostram a ocorrência de 100-200 fibras no ramo zigomático do nervo facial e 834±285 no ramo bucal do nervo facial. Esses valores excedem a proporção de 2:1 que Coombs et al. (2009) menciona em seu estudo. O diâmetro médio do nervo massetérico foi de 0,75 ± 0,18 mm, o que está de acordo com o proposto por

Cotrufo et al. (2011) que se refere ao diâmetro de 0,6 mm como bom para a reanimação masseterico-facial.

Dividimos as fibras do NM em três grupos (fibras pequenas <10 μm², fibras médias 10-20 μm² e fibras grandes> 20 μm²) (Ramkumar et al., 2015). Encontramos 12,50% de fibras pequenas, 9,33% de médio e 78,17% de fibras grandes baseadas na área total da fibra nervosa. Ramkumar et al. (2015) relataram a presença de 8,83% de fibras pequenas, 30,39% de médias e 60,78% de fibras grandes no nevo abducente. Eles também relataram 17,95%, 35,9% e 46,15% para os mesmos grupos no nervo troclear.

O diâmetro da fibra foi utilizado para fazer associações funcionais de acordo com a classificação de Erlanger e Gasser. Nesta classificação, as fibras motoras Aα possuem diâmetro maior que 12 μm, as fibras Aβ possuem diâmetro entre 5-12 μm, as fibras Aγ têm diâmetro menor que 5 μm (Parent, 1996). O diâmetro das fibras mielinizadas do NM variou de 1,49 μm a 13,25 μm, podendo estar associado à fibra nervosa intrafusal γ (21,08%), fibra nervosa intra e extrafusal β (77,05%) e fibra nervosa extrafusal α (1,9%).

Os nervos cranianos podem apresentar um número maior de fibras proprioceptivas (Abo-El-Enene, 1978), o que justifica ter uma soma maior de fibras pequenas e médias do que as descritas em nosso estudo. Estas fibras pequenas e médias teriam um diâmetro estimado até 5 μm, o que é compatível com as fibras γ. As fibras grandes são compatíveis com o diâmetro estimado das fibras β (5-12 mm) e α (> 12 mm), que fornecem fibras intrafusais e extrafusais.

A área axonal média foi de 12,98 ± 11,48 μm². Sharma et al. (2009) relataram a média de 9,71±0,71 μm² em nervo oculomotor para cadáveres acima de 71 anos. Ramkumar et al. (2015) mostra 19,45±2,64 μm² de área axonal em nervo troclear e 23,72±6,01 μm² em nervo abducente para pessoas acima de 60 anos.

A espessura média da bainha de mielina encontrada em nosso estudo foi de 1,98±0,82 µm. Sharma et al. (2009) reportaram que a média da bainha de mielina em nervo oculomotor de cadáveres foi de 2,06±0,33 µm para pessoas acima de 71 anos, enquanto que Ramkumar et al. (2015) mostraram valores de espessura média de mielina de 2,48±0,39 µm em nervo troclear e 2,90±0,51 µm em nervo abducente para indivíduos acima de 60 anos. Comparando esses resultados com categorias mais jovens, esses autores demonstram que a espessura da mielina parece ter aumentado com a idade. Nossos dados demonstraram essa mesma tendência. A espessura da mielina do nervo troclear humano aparentemente aumenta com a idade provavelmente devido à adição de novas lamelas (Peters, 2002). Assim, pode-se sugerir que os perfis de mielina irregulares e as alterações do tecido conjuntivo na idade avançada podem ser devido ao fator de crescimento nervoso alterado ou outros fatores semelhantes que precisam de confirmação adicional usando marcadores bioquímicos específicos.

A média do g-ratio em nosso estudo foi de 0,48 ± 0,11, variando de 0,2 a 0,81. Thomas e Ochoa (1984) citaram ainda que os valores de g-ratio inferiores a 0,4 indicam a presença de fibras nervosas degeneradas com espessamento anormal da bainha de mielina, enquanto valores acima de 0,7 indicam fibras regeneradas com bainha de mielina mais fina ou fibras nervosas desmielinizadas.

De Campos et al. (2015) relataram, no nervo laríngeo recorrente, g-ratio variando de 0,61±0,01 a 0,68±0,05. Páfaro et al. (2018) para o nervo hipoglosso comparou o lado esquerdo (0,90±0,1) com o lado direito (0,88±0,1) e constatou que não há diferença estatisticamente significante entre os dois. Para nervos periféricos, como o nervo ciático, Ugrenovic et al. (2015) demonstraram que o g-ratio variou de 0,7 a 0,9 em pessoas de 60 a 80 anos.

Devido à heterogeneidade de nossa amostra, não pudemos analisar estatisticamente se existem diferenças significativas nas análises apresentadas entre homens e mulheres ou comparar o g-ratio entre diferentes idades. Pudemos ver que, no indivíduo com menos de 60 anos de idade, o g-ratio estava dentro dos valores ótimos para o grau de mielinização. No entanto, os dados são importantes devido à escassez de informações sobre o nervo massetérico na literatura. Estudos futuros podem corroborar esses dados e estabelecer melhores relações entre diferentes gêneros e faixas etárias.

Conseguimos identificar uma região anatômica de localização do nervo massetérico em cadáveres humanos, seu padrão de ramificação e sua relação topográfica com a artéria massetérica. Esses dados podem contribuir para facilitar a abordagem clinico - cirúrgica do nervo massetérico e minimizar o risco de lesões vasculares. Além disso, dados morfométricos microscópicos do nervo massetérico foram descritos e também seu potencial de neuroreanimação. Esses dados fornecem embasamento para o possível uso do nervo massetérico como doador em anastomoses com o nervo facial em indivíduos que são acometidos por algum tipo de paralisia da musculatura da mímica da face.

5. CONCLUSÃO

Nos cadáveres estudados, o nervo massetérico, a partir da fossa infratemporal, cruzou a incisura mandibular, anteriormente e superiormente à artéria massetérica e sequencialmente emitiu de 1 a 3 ramos para suprir o músculo masseter. O ponto de cruzamento pela incisura apresentou profundidade de 1,1 cm e posicionamento de aproximadamente 3,3 cm anterior ao trago e 0,8 cm inferior ao arco zigomático. O nervo massetérico foi identificado como sendo monofascicular com 1683±315 fibras nervosas mielínicas e com diâmetro médio de 0,76±0,18 mm. A área média das fibras foi de 51,85 μm², com diâmetro médio de 7,65 μm sendo a maioria (61,64%) com diâmetro entre 5 e 12 μm, espessura média da bainha de mielina de cerca de 1,98 μm e com alto grau de mielinização (g-ratio=0,48).

Este estudo é o primeiro que descreve a anatomia macroscópica e microscópica do nervo massetérico em amostras caucasianas brasileiras. Os dados obtidos neste estudo contribuem para a identificação de uma região de localização do nervo massetérico para acesso cirúrgico e fornecem dados morfométricos microscópicos para nortear procedimentos de anastomose massetérico-facial em correções cirúrgicas de paralisias da musculatura da mímica facial.

6. REFERÊNCIAS BIBLIOGRÁFICAS

1. Abo-El-Enene, M. A. (1978). Proprioceptive afferent fibers in the cranial nerves III, IV and VI. Cells Tissues Organs, 101(1), 62–65.

2. Angspatt, A., & Pannanusorn, C. (2018). The masseteric nerve: An anatomical study in Thai population with an emphasis on its use in facial reanimation. Asian Journal of Surgery, 41(5), 486–489.

3. Bear, M. F., Connors, B. W., & Paradiso, M. A. Neurociências: Desvendando o sistema nervoso. 2ª ed. Porto Alegre: Artmed, 2002.

4. Benecke, J.E.Jr. (2002). Facial Paralysis. Otolatyngol Clin North Am, 33, 357–365.

5. Bermudez, L., & Nieto, L. (2004). Masseteric-Facial Nerve Anastomosis: Case Report. Journal of Reconstructive Microsurgery, 21(01), 25–30.

6. Bianchi, B., Varazzani, A., Pedrazzi, G., Poddi, V., Ferrari, S., Brevi, B., & Ferri, A. (2018). Masseteric cooptation and crossfacial nerve grafting: Is it still applicable 22 months after the onset of facial palsy? Microsurgery, 1–7.

7. Biglioli, F., Soliman, M., El-Shazly, M., Saadeldeen, W., Abda, E. A., Allevi, F., & Califano, L. (2018). Use of the masseteric nerve to treat segmental midfaceparesis. British Journal of Oral and Maxillofacial Surgery, 1–8.

8. Biglioli, F., Colombo, V., Rabbiosi, D., Tarabbia, F., Giovanditto, F., Lozza, A., & Mortini, P. (2017). Masseteric–facial nerve neurorrhaphy: results of a case series. Journal of Neurosurgery, 126(1), 312–318.

9. Biglioli, F., Frigerio, A., Colombo, V., Colletti, G., Rabbiosi, D., Mortini, P., & Brusati, R. (2012). Masseteric–facial nerve anastomosis for early facial reanimation. Journal of Cranio-Maxillofacial Surgery, 40(2), 149–155.

10. Bolat, D., Yıldız, D., Bahar, S., Yürüker, S., Kaymaz, F., Ilgın, C., & Sabancı, S. (2017). A comparative study of oculomotor, trochlear and abducens nerves in Arabian foals. Biotechnic & Histochemistry, 92(2), 149–156.

11. Borschel, G. H., Kawamura, D. H., Kasukurthi, R., Hunter, D. A., Zuker, R. M., & Woo, A. S. (2012). The motor nerve to the masseter muscle: An anatomic and histomorphometric study to facilitate its use in facial reanimation. Journal of Plastic, Reconstructive & Aesthetic Surgery, 65(3), 363–366.

12. Brenner, E., & Schoeller, T. (1998). Masseteric nerve: A possible donor for facial nerve anastomosis? Clinical Anatomy, 11(6), 396–400.

13. Cardenas-Mejia, A., & Palafox, D. (2018). Facial reanimation surgery in Möbius syndrome: Experience from 76 cases from a tertiary referral hospital in Latin America. Annales de Chirurgie Plastique Esthétique, 63(4), 338–342.

14. Carter., G. M., & Harkness, E. M. (1995). Alterations to Mandibular Form Following Motor Denervation of the Masseter Muscle. An experimental Study in Rat. Journal Anatomy, 186, 541–548.

15. Cattaneo, L., Saccani, E., De Giampaulis, P., Crisi, G., & Pavesi, G. (2010). Central facial palsy revisited: A clinical-radiological study. Annals of Neurology, 68(3), 404–408.

16. Cha, C. I., Hong, C. K., Park, M. S., & Yeo, S. G. (2008).Comparison of Facial Nerve Paralysis in Adults and Children. Yonsei Medical Journal, 49(5), 725–734.

17. Cheng, A., Audolfsson, T., Rodriguez-Lorenzo, A., Wong, C., & Rozen, S. (2013). A reliable anatomic approach for identification of the masseteric nerve. Journal of Plastic, Reconstructive & Aesthetic Surgery, 66(10), 1438–1440.

18. Chomiak, T., & Hu, B. (2009). What Is the Optimal Value of the g-Ratio for Myelinated Fibers in the Rat CNS? A Theoretical Approach. PLoS ONE, 4(11), e7754.

19. Chuang, D. C.-C., Lu, J. C.-Y., Chang, T. N.-J., & Laurence, V. G. (2018). Comparison of Functional Results After Cross-Face Nerve Graft-, Spinal Accessory Nerve-, and Masseter Nerve-Innervated Gracilis for Facial Paralysis Reconstruction. Annals of Plastic Surgery, 1–9.

20. Collar, R. M., Byrne, P. J., & Boahene, K. D. O. (2013). The Subzygomatic Triangle. Plastic and Reconstructive Surgery, 132(1), 183–188.

21. Coombs, C. J., Ek, E. W., Wu, T., Cleland, H., & Leung, M. K. (2009). Masseteric-facial nerve coaptation – an alternative technique for facial nerve reinnervation. Journal of Plastic, Reconstructive & Aesthetic Surgery, 62(12), 1580–1588.

22. Corrales, C. E., Gurgel, R. K., & Jackler, R. K. (2012). Rehabilitation of Central Facial Paralysis With Hypoglossal-Facial Anastomosis. Otology & Neurotology, 33(8), 1439–1444.

23. Cotrufo, S., Hart, A., Payne, A. P., Sjogren, A., Lorenzo, A., & Morley, S. (2011). Topographic anatomy of the nerve to masseter: An anatomical and clinical study. Journal of Plastic, Reconstructive & Aesthetic Surgery, 64(11), 1424–1429.

24. De Campos, D., Xavier, L. L., Goulart, G. R., Thomaz, L. D. G. R., Malysz, T., & Jotz, G. P. (2015). Similarities in the surface area/volume ratio in the fibers of the recurrent laryngeal nerve can explain the symmetry in the vocal fold mobility? Medical Hypotheses, 85(6), 989–991.

25. Doménech Juan, I.,Tornero, J., Cruz Toro, P., Ortiz Laredo, N., Vega Celiz, J., Junyent, J., & MañosPujol, M. (2014). Cirugía reparadora de la parálisis facial mediante colgajo libre microvascularizado de músculo gracilis. Acta Otorrinolaringológica Española, 65(2), 69–75.

26. Donnarumma, P., Tarantino, R., Gennaro, P., Mitro, V., Valentini, V., Magliulo, & G., Delfini, R. (2014). Penetrating Gunshot Wound to the Head: Transotic Approach to Remove the Bullet and Masseteric-Facial Nerve Anastomosis for Early Facial Reanimation. Turk Neurosurg, 24(3), 415–148.

27. Fournier, H.D., Denis, F., Papon, X., Hentati, N., & Mercier, P. (1997). An anatomical study of the motor distribution of the mandibular nerve for a masseteric-facial anastomosis to restore facial function. Surgical and Radiologic Anatomy, 19(4), 241–244.

28. Graça, D. L. (1988). Mielinização, desmielinização e remielinização do Sistema Nervoso Central. Arq. Neuro-Psiquiat, 46(3), 292–297.

29. Heimer, L. The Human Brain and the Spinal Cord. 2nded. New York: Springer-Verlag, 1994.

30. Holtmann, L. C., Eckstein, A., Stähr, K., Xing, M., Lang, S., & Mattheis, S. (2017). Outcome of a graduated minimally invasive facial reanimation in patients with facial paralysis. European Archives of Oto-Rhino-Laryngology, 274(8), 3241–3249.

31. Hontanilla, B., & Cabello, A. (2016). Spontaneity of smile after facial paralysis rehabilitation when using a non-facial donor nerve. Journal of Cranio-Maxillofacial Surgery, 44(9), 1305–1309.

32. Hontanilla, B., & Marre, D. (2015). Masseteric-facial nerve transposition for reanimation of the smile in incomplete facial paralysis. British Journal of Oral and Maxillofacial Surgery, 53(10), 943–948.

33. Hwang, K., Kim, Y. J., Chung, I. H., & Song, Y. B. (2005). Course of the Masseteric Nerve in Masseter Muscle. Journal of Craniofacial Surgery, 16(2), 197–200.

34. Ikeda, M., & Oka, Y. (2012). The relationship between nerve conduction velocity and fiber morphology during peripheral nerve regeneration. Brain and Behavior, 2(4), 382–390.

35. Isolan G.R., Pereira A.H., Pires de Aguiar P.H., Antunes A.C.M., Mousquer J.P., & Pierobon M.R. (2012) Anatomia microcirúrgica da artéria carótida externa: um estudo estereoscópico. J Vasc Bras; 11(1):3–11.

36. Jotz, G. P., Marrone, A. C. H., Stefani, M. A., Bizzi, J. J. & Aquini, M. G. Neuroanatomia Clínica e Funcional. 1ª ed. Porto Alegre: Elsevier, 2017.

37. Kaya, B., Apaydin, N., Loukas, M., & Tubbs, R. S. (2014). The topographic anatomy of the masseteric nerve: A cadaveric study with an emphasis on the effective zone of botulinum toxin A injections in masseter. Journal of Plastic, Reconstructive & Aesthetic Surgery, 67(12), 1663–1668.

38. Kerns, J. M. (1980) Postnatal differentiation of the rat thochlear nerve. Jouranl of Comparative Neurology, 189, 291–306.

39. Klebuc, M., & Shenaq, M. (2004). Donor Nerve Selection in Facial Reanimation Surgery. (2004). Seminars in Plastic Surgery, 18(1), 53–59.

40. Lifchez, S. D., Matloub, H. S., & Gosain, A. K. (2005). Cortical adaptation to restoration of smiling after free muscle transfer innervated by the nerve of masseter. Plast Reconstr Surg, 115, 1472–1479.

41. Magden O., Göçmen-Mas N., Senan S., Edizer M., Karaçayli U., & Karabekir H.S. (2009) The premasseteric branch of facial artery: its importante in craniofacial surgery. Turk Neurosurg; 19(1):45–50.

42. Malysz, T., Ilha, J., Nascimento, P. S., De Angelis, K., Schaan, B. D., & Achaval, M. (2010). Beneficial effects of treadmill training in experimental diabetic nerve regeneration. Clinics, 65(12), 1329–1337.

43. Manktelow, R. T., Tomat, L. R., Zuker, R. M., & Chang, M. (2006). Smile Reconstruction in Adults with Free Muscle Transfer Innervated by the Masseter Motor Nerve: Effectiveness and Cerebral Adaptation. Plastic and Reconstructive Surgery, 118(4), 885–899.

44. Manni, J. J., Beurskens, C. H. G., van de Velde, C., & Stokroos, R. J. (2001). Reanimation of the paralyzed face by indirect hypoglossal-facial nerve anastomosis. The American Journal of Surgery, 182, 268–273.

45. Manzano, G.M., Giuliano, L.M.P. Nóbrega, & J.A.M. (2008). A breif historical note on the classification of nerve fibers. Arq Neuropsiquiatr, 66(1), 117–119.

46. Moore, Keith L. Anatomia orientada para a clínica. 7. ed. Rio de Janeiro: Guanabara Koogan, 2014.

47. Moturi, S. (2014). To Evaluate the Feasibility of Neurotisation of Facial Nerve Branches with Ipsilateral Masseteric Nerve: An Anatomic Study. Journal of Clinical and Diagnostic Research, 8(4), 4–7.

48. Netter, FH. Atlas de Anatomia Humana. 2nd ed. Porto Alegre: Artmed; 2000:35

49. Novas, R. B., Fazan, V. P. S., & Felipe, J. C. (2015). A New Method for Automated Identification and Morphometry of Myelinated Fibers Through Light Microscopy Image Analysis. Journal of Digital Imaging, 29(1), 63–72.

50. Owusu, J. A., Truong, L., & Kim, J. C. (2016). Facial Nerve Reconstruction With Concurrent Masseteric Nerve Transfer and Cable Grafting. JAMA Facial Plastic Surgery, 18(5), 335–339.

51. Páfaro, J. N., Goulart, G. R., Silveira, C. H., Cella, P. A. M., Malysz, T., Jotz, G. P., & Campos, D. (2018). Degree of Myelination (g-ratio) of the Human Hypoglossal Nerve. Journal of Morphological Sciences, 35(01), 25–27.

52. Parent, A. Carpenter's human neuroanatomy. 9thEd. Batltimore: Williams & Wilkins, 1996.

53. Purves, D., Augustine, G. J. Fitzpatrick, D., Hall, W. C., Lamantia, A. McManara, J. O. & White. L. E. Neurociências. 4ª Ed. Artmed, 2010.

54. Parker, N.P. (2012). Orthodromic Temporalis Tendon Transfer. Archives of Facial Plastic Surgery; 14(1):39–44

55. Peters, G.B. 3rd, Bakri, S.J., & Krohel, G.B. (2002). Cause and Prognosis of nontraumatic sixth nerve palsies in young adults. Ophthalmology, 109: 1925–1928.

56. Placheta, E., Tinhofer, I., Schmid, M., Reissig, L. F., Pona, I., Weninger, W., & Tzou, C. H. (2016). The Spinal Accessory Nerve for Functional Muscle Innervation in Facial Reanimation Surgery. Annals of Plastic Surgery, 77(6), 640–644.

57. Poddar, R., Bhattacharya, A., Sinha, & I. Ghosal, A. K. (2017). An Anatomical study for localisation of Zygomatic branch of Facial nerve and Masseteric nerve - An aid to nerve coaptation for facial reanimation surgery: A cadaver based study in Eastern India. Indian Journal of Plastic Surgery, 50(1), 74–78.

58. Rajab, B.M., Sarraf, A.A., Abubaker, A.O., & Laskin, D.M. (2009). Masseteric Artery: Anatomic Location and Relationship to the Temporomandibular Joint Area. Journal of Oral and Maxillofacial Surgery; 67(2):369–371.

59. Ramkumar, M., Sharma, S., G. Jacob, T., N. Bhardwaj, D., C. Nag, T., & Sankar Roy, T. (2015). The Human Trochlear and Abducens Nerves at Different Ages - a Morphometric Study. Aging and Disease, 6(1), 6–16.

60. Rowlerson, A., Raoul, G., Daniel, Y., Close, J., Maurage, C.-A., Ferri, J., & Sciote, J. J. (2005). Fiber-type differences in masseter muscle associated with different facial morphologies. American Journal of Orthodontics and Dentofacial Orthopedics, 127(1), 37–46.

61. Rushton, W.A. (1951) A theory of the effects of fibre size in medullated nerve. J Physiol 115(1):101–122.

62. Schenk, H. C., Haastert-Talini, K., Jungnickel, J., Grothe, C., Meyer, H., Rehage, J., & Tipold, A. (2014). Morphometric Parameters of Peripheral Nerves in Calves Correlated with Conduction Velocity. Journal of Veterinary Internal Medicine, 28(2), 646–655.

63. Sharma, S., Ray, B., Bhardwaj, D., Dwivedi, A. K., & Roy, T. S. (2009). Age changes in the human oculomotor nerve – A stereological study. Annals of Anatomy - Anatomischer Anzeiger, 191(3), 260–266.

64. Socolovsky, M., Martins, R. S., di Masi, G., Bonilla, G., & Siqueira, M. (2016). Treatment of complete facial palsy in adults: comparative study between direct hemihypoglossal-facial neurorrhaphy, hemihipoglossal-facial neurorrhaphy with grafts, and masseter to facial nerve transfer. Acta Neurochirurgica, 158(5), 945–957.

65. Suwa, F., Takemura, A., Ehara, Y., Takeda, N., & Masu, M. (1990). On the arteriamaxillaris which passes medial to the pterygoideuslateralis muscle of the Japonese patterns of origin of the inferior alveolar, the masseteric and the posterior temporal arteries. Okajimas Folia AnatJpn; 67(5):303–308.

66. Suzuki, T. (1989). Arterial supply to the masseter muscle in the rat. Kaibogakuzasshi; 64(1):8–17.

67. Thomas, P.K., & Ochoa, J. (1984). Microscopic anatomy of the peripheral nervous system. In: Dyck PJ, Thomas PK (eds) Peripheral neurophathy, 2nd edn. Saunders, London, pp 39–91.

68. Toure, G. (2018). Arterial Vascularization of the Mandibular Condyle and Fractures of the Condyle. Plastic and Reconstructive Surgery; 141(5):718e–725e.

69. Waxman, S. G. (1980). Determinants of conduction velocity in myelinated nerve fibers. Muscle Nerve 3:141–150.

70. Ugrenović, S., Jovanović, I., Vasović, L., Kundalić, B., Čukuranović, R., & Stefanović, V. (2015). Morphometric analysis of the diameter and g-ratio of the myelinated nerve fibers of the human sciatic nerve during the aging process. Anatomical Science International, 91(3), 238–245.

71. West, K. L., Kelm, N. D., Carson, R. P., & Does, M. D. (2016). A revised model for estimating g-ratio from MRI. NeuroImage, 125, 1155–1158.

72. Won, S.Y., Choi, D.Y., Kwak, H.H., Kim, S.T., Kim, H.J., & Hu, K.S. (2011). Topography of the arteries supplying the masseter muscle: Using dissection and Sihler's method. Clinical Anatomy;25(3):308–313.

73. Wysocki, J., Reymond, J., & Krasucki, K. (2012) Vascularization of the mandibular condylar head with respect to intracapsular fractures of mandible. Journal of Cranio-Maxillofacial Surgery; 40(2):112–115.

74. Yoshioka, N. (2017). Differential Reanimation of the Midface and Lower Face Using the Masseteric and Hypoglossal Nerves for Facial Paralysis. Operative Neurosurgery, 15(2), 174–178.

75. Yoshioka, N. (2016). Masseter Atrophication after Masseteric Nerve Transfer. Is It Negligible? Plastic and Reconstructive Surgery - Global Open, 4(4), e692.

76. Yoshioka, N. (2016). Masseteric Nerve as “Baby Sitter” Procedure in Incomplete Facial Paralysis. Plastic and Reconstructive Surgery - Global Open, 4(4), e669.

77. Yoshioka, N., & Tominaga, S. (2015). Masseteric nerve transfer for short-term facial paralysis following skull base surgery. Journal of Plastic, Reconstructive & Aesthetic Surgery, 68(6), 764–770.

78. Zamanlu, M., Khamnei, S., SalariLak, S., Oskoee, S. S., Shakouri, S. K., Houshyar, Y. & Salekzamani, Y. (2012). Chewing side preference in the first and all mastication cycles for hard and soft morsels. Int J Clin Exp Med, 5(4): 326–331.